17(S 6)

HONG KONG MEDICAL JOURNALS

香港醫學雜誌

Volume 17 ■ Number 6 ■ December 2011

Supplement 6

HONG KONG SUPPLEMENT 6
VOLUME 17 ■ NUMBER 6 ■ DECEMBER 2011

HONG KONG MEDICAL JOURNAL
香港醫學雜誌

The official publication of the
Hong Kong Academy of Medicine
and the Hong Kong Medical Association

Research Fund for the Control of Infectious Diseases
Health and Health Services Research Fund
Health Services Research Fund
Research Dissemination Reports

控制傳染病研究基金
衞生及醫護服務研究基金
醫療服務研究基金
研究成果報告

Health Care Delivery
醫護服務的提供

Health Services Research
醫療服務研究

Respiratory Infectious Diseases
呼吸道感染疾病

Viral Hepatitis
病毒性肝炎

香港醫學專科學院出版社
HONG KONG ACADEMY OF MEDICINE PRESS

HONG KONG MEDICAL JOURNAL
香港醫學雜誌

Vol 17 No 6 December 2011
Supplement 6

Viral Hepatitis

Dissemination reports are concise informative reports of health-related research supported by funds administered by the Food and Health Bureau, namely the *Research Fund for the Control of Infectious Diseases* (RFCID), the *Health and Health Services Research Fund* (HHSRF), and the *Health Services Research Fund* (HSRF). This issue contains 10 dissemination reports of funded projects related to health care delivery, health services research, respiratory infectious diseases, and viral hepatitis. In particular, three projects are highlighted due to their potentially significant findings, impact on health care delivery and practice, and/or contribution to health policy formulation in Hong Kong.

Currently, over one-third of the world's population is affected by hepatitis B (HBV) and hepatitis C (HCV) infection. In Hong Kong the prevalence of hepatitis B seropositivity in the adults is between 4 and 10%. A significant proportion of these individuals go on to develop chronic hepatitis, but it is unclear which subgroups are at risk and will develop its related complications. Huang et al[1] conducted a thorough literature review to determine whether specific HBV or HCV genotypes influenced progression to hepatocellular carcinoma (HCC). The data indicated that HBV genotypes A and C conferred increased risk for development of HCC, whereas HBV genotypes B and D were associated with a slightly reduced risk. Similarly, HCV genotype 1b was associated with a significantly increased risk of developing HCC. Knowing which genotype predisposes patients to hepatic carcinogenesis can help to better target populations for monitoring and/or early intervention, potentially improving early diagnosis and prolong life.

Emerging infectious diseases have posed a significant threat to human health. During late 2002 and early 2003, severe acute respiratory syndrome (SARS) first occurred in Guangdong province, China, and subsequently spread to many other countries. The potential for further outbreaks was curtailed by closure and depopulation of wild animal markets in early 2004. A novel coronavirus, SARS-coronavirus (SARS-CoV) was identified as the aetiological agent responsible for the initial outbreak. Chen et al[2] conducted an analysis of samples collected during the 2003 SARS outbreak supplemented with systematic virological surveillances of coronavirus in bats and other wild animals between 2004 and 2007, with a view to identifying the natural reservoir of SARS-CoV. After exhaustive studies they identified bats as the natural reservoir for coronaviruses, including SARS-CoV, that affect humans and animals. However, the immediate precursor of SARS-CoV remains unknown. The authors call for continued surveillance and note the potential risk posed by live animal markets in the dissemination of disease.

Evaluation of health-related quality of life (QoL) in young children (aged <5 years) with cancer mainly relies on proxy assessments performed by nurses or parents, both of which are subject to bias. Most children over 3 years old have the capacity to respond in meaningful and reliable ways, provided that they are assessed in an age-appropriate manner. This would enable direct QoL assessment. Fielding et al[3] set out to develop an age-appropriate direct assessment of QoL in 3 to 5 years old children with cancer, and to validate its use in 5 to 8 years old cancer children of southern Chinese cultural background. They found that the direct measurement of QoL in young children aged 30 to 72 months was feasible and valid, which may enhance cancer care in this vulnerable population.

We hope you will enjoy this selection of research dissemination reports. Electronic copies can be downloaded from the Research Fund Secretariat website (**http://www.fhb.gov.hk/grants**). Researchers interested in the funds administered by the Food and Health Bureau may also visit the website for detailed information about application procedures.

Supplement co-editors

Dr Jenny Lam
Associate Consultant
(Research Office)
Food and Health Bureau

Dr Richard A Collins
Scientific Review Director
(Research Office)
Food and Health Bureau

References

1. Huang JQ, Zheng GF, Lai CL, Yuen MF, Wong BC. Risk of liver cancer in patients with hepatitis B or C. Hong Kong Med J 2011;17(Suppl 6):41-3.
2. H Chen, Y Guan, X Fan. Animal reservoirs for SARS-like coronavirus in southern China. Hong Kong Med J 2011;17(Suppl 6):36-40.
3. Fielding R, Chan GC, Lam WW. Health-related quality of life assessment for Hong Kong Chinese children with cancer. Hong Kong Med J 2011;17(Suppl 6):13-6.

EML Wong 黃美玲
TH Rainer 譚偉恩
YC Ng 伍凝珠
MS Chan 陳民秀
V Lopez 羅考思

Cost- ffectiveness of Dermabond versus sutures for lacerated wound closure: a randomised controlled triale

Key Messages

1. For management of simple lacerated wounds, tissue adhesive (Dermabond) achieved more positive outcomes but incurred higher cost, compared with standard sutures.
2. Dermabond may be more cost-effective than standard sutures from a societal viewpoint.
3. Use of sutures required more nursing time and additional costs from subsequent dressing, whereas use of Dermabond incurred higher equipment costs.
4. Dermabond achieved better appearance outcome and patient satisfaction, compared with sutures.
5. Pain levels were not significantly different in patients treated with Dermabond or sutures.

Hong Kong Med J 2011;17(Suppl 6):S4-8

The Nethersole School of Nursing, The Chinese University of Hong Kong
EML Wong
Accident and Emergency Medicine Academic Unit, The Chinese University of Hong Kong
TH Rainer, MS Chan
Department of Economics, Hong Kong Baptist University
YC NG
School of Nursing (NSW and ACT), Australian Catholic University, Australia
V Lopez

HHSRF project number: 03040071

Principal applicant and corresponding author:
Dr Eliza Mi-Ling Wong
The Nethersole School of Nursing, Room 824, Esther Lee Building, The Chinese University of Hong Kong
Tel: (852) 2609 8098
Fax: (852) 2603 5935
Email: elizawong@cuhk.edu.hk

Introduction

In Hong Kong, nearly 3500 wound closures are handled by each accident and emergency department (AED) each year.[1] Suturing is a painful procedure and requires competent skill and follow-up visits for suture removal.[2,3] Dermabond (2-octyl cyanoacrylate) is a tissue adhesive used as a wound closure alternative.[2-5] Dermabond and sutures achieve equivalent healed wound appearance, but Dermabond entails a shorter procedure time and results in greater patient satisfaction than sutures.[2,3] We aimed to compare Dermabond versus standard wound sutures in terms of cost-effectiveness, outcome appearance, infection rate, pain, and satisfaction.

Methods

This randomised, unblinded, controlled study was conducted from 1 October 2005 to 30 September 2006. Patients from AEDs of two regional hospitals of Hong Kong who were aged ≥18 years, ambulatory, and had simple laceration wound of <8 cm were invited to participate. Patients with complicated wounds, scalp wounds, physical, visual or cognitive impairment were excluded. Patients were randomly assigned to either the control group (wound closure by sutures using standard nylon stitches) or experimental group (wound closure by tissue adhesive—Dermabond). Wound closure was defined as the process of realigning lacerated tissue plane. An intention-to-treat method was used for analysis.

Wounds were disinfected. For the suture group, the wound was anaesthetised with lignocaine 1% and sutured using standard nylon stitiches by AED nurses. After wound closure, simple dressings (plain gauze or band aid) was applied to cover the wound until removal. On discharge, a wound care instruction sheet was provided, and an out-patient follow-up was arranged for suture removal (or dressing as necessary).

For the Dermabond group, no local anaesthetic agent was used. Dermabond was gently 'painted' on the wound sites by AED nurses, and the wound edges were held together for at least 30 seconds to ensure adequate polymerisation. On discharge, a wound care instruction sheet was provided. No wound follow-up was arranged. Clinical data of the patients was recorded by the research assistant at three time points: day 14, month 1, and month 3.

A wound evaluation score (WES) was used to assess six clinical variables: absence of step off, contour irregularities, wound margin separation, edge inversion, excessive distortion, and overall cosmetic appearance. The total WES was derived by the addition of the 'yes' responses to the six variables; a score of six indicates optimal and <6 as sub-optimal wound appearance.[4]

A visual analogue cosmesis scale (VACS) was used to assess each patient's degree of satisfaction with wound appearance outcome after suture removal, with 0 indicating least satisfied and 100 most satisfied. A visual analogue scale (VAS) was used to assess the level of pain during the wound closure process, with 0 indicating least pain and 100 most pain.

A wound infection tool was used to derive a wound score, which was calculated by a reviewer for wound separation, and exudates or erythema from the line of the incision. A score of 0 indicated normal healing and 30 complete dehiscence of the wound.

The patient satisfaction for the overall wound management process was also assessed using a scale of 0 (least satisfied) to 100 (most satisfied). In addition, analgesic consumption at home, rate of wound follow-up, and adverse reactions after wound closure were recorded.

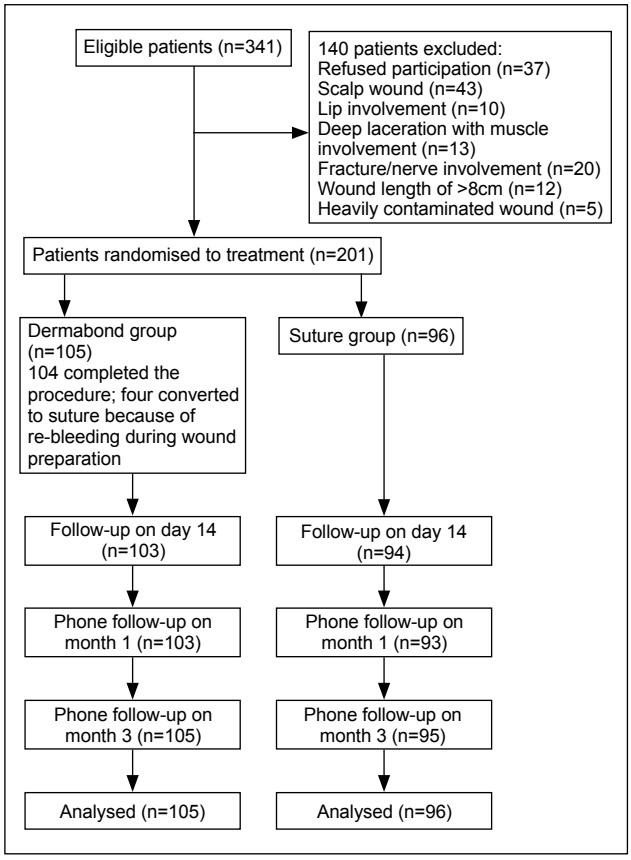

Fig 1. Flow chart of patient randomisation

The total costs of both treatments were compared. All activities related to the treatment or subsequent unexpected outcomes for each patient were recorded. A full cost (total doctor and nursing time of the whole procedure, actual cost of materials, analgesic consumption) for each patient was calculated. The costs for the suture and Dermabond groups were compared for cost-effectiveness analysis. Based on a hospital perspective, incremental cost-effective ratio was used.

Results

Of 201 patients, 105 were treated with Dermabond and 96 with sutures (Fig 1). There was no significant difference between groups in terms of age, gender, co-existing illness, and baseline variables of pain level, mechanism of injury, injury site, wound length, and time from injury to presentation (Table 1).

At day 14, more percentage of patients in the Dermabond group achieved the optimal WES (89.5% vs 86.5%, P=0.29, Table 2). The difference was significant when using VACS perceived by the reviewer (79.1 vs 66.5, P<0.005, t test).

At month 3, using VACS as the dependent variable with potential confounders (such as sex, age, wound length, wound life, and baseline appearance score), multiple regression analysis showed that only wound length had a significant effect on VACS (effect= –2.88, standard error=0.91, P=0.002). Repeated measure ANOVA was used to test the group difference in terms of VACS perceived by the participants at the four time points. There was a significant main effect for intervention (f (1,198)=8.6, P=0.004); the Dermabond group had significantly higher mean score than the suture group (83.3 vs 75 at day 14, 89.3 vs 81 at month 1, and 92.5 vs 85.4 at month 3 (P<0.001, Table 2, Fig 2).

Table 1. Baseline characteristics

Variable	All patients (n=201)	Dermabond group (n=105)	Suture group (n=96)
No. (%) of patients from hospital A	112 (56)	58 (55)	54 (56)
No. (%) of patients from hospital B	89 (44)	47 (45)	42 (44)
Mean±SD patient age (years)	42.7±19.1	43±19.4	42.5±18.9
No. (%) of males	138 (68.7)	71 (67.6)	67 (69.8)
No. (%) of patients with diabetes mellitus	8 (4.0)	4 (3.8)	4 (4.2)
Median (IQR) time from injury to presentation (minutes)	44 (30-61)	43 (30-58)	45 (32.5-64)
Mechanisms of injury (No. [%] of patients)			
Contusion	32 (15.9)	19 (18.1)	13 (13.5)
Cut	115 (57.2)	63 (60)	52 (54.2)
Falls	43 (21.4)	17 (16.2)	26 (27.1)
Motor vehicle accident	2 (1.0)	2 (1.9)	0 (0)
Sports	9 (4.5)	4 (3.8)	5 (5.2)
Site of injury (No. [%] of patients)			
Face	89 (44.3)	51 (48.6)	38 (39.6)
Hand	85 (42.3)	42 (40)	43 (44.8)
Lower limb	12 (6.0)	5 (4.8)	7 (7.3)
Upper limb	13 (6.5)	6 (5.7)	7 (7.3)
Chest	2 (1.0)	1 (1.0)	1 (1.0)
Median (25th-75th quartiles) wound length (cm)	1.7 (1-2)	1.5 (1-2)	2.0 (1-2)

Table 2. Outcome measures between two groups at different time points

Variable	Dermabond group	Suture group	Absolute difference (95% CI)	P value
Visual analogue cosmesis scale score (mean [95% CI])				
Baseline (after wound closure)	60.8 (60.2-61.5)	62.3 (61.3-63.3)	1.5 (0.4-3.5)	-
Day 14	83.3 (79.6-87.0)	75.0 (71.3-78.5)	8.3 (3.7-13.7)	-
Day 14 (assessed by research assistant)	79.1 (75.5-84.4)	66.5 (60.6-70.2)	15.5 (8.3-22.2)	<0.001*
Month 1	89.3 (86.1-92.6)	80.9 (77.6-84.3)	8.4 (4.0-12.7)	-
Month 3	92.5 (89.9-95.1)	85.4 (82.8-88.1)	7.1 (3.4-10.8)	-
Mean difference (baseline vs month 3) [mean±SD]	30.7±14	23.3±14	-	<0.001*
Appearance complication at day 14 using wound evaluation score (WES) [No. (%) of patients]				
Step of	3 (2.9)	1 (1.1)	-	0.34†
Contour irregularities	1 (0.95)	2 (2.1)	-	0.47†
Wound margin separation of >2 mm	2 (1.9)	6 (6.4)	-	0.11†
Edge inversion	1 (1.0)	2 (2.1)	-	0.49†
Excessive distortion	2 (1.9)	2 (2.1)	-	0.66†
Overall sub-optimal cosmetic appearance	8 (7.8)	10 (10.4)	-	0.34†
Suboptimal wound (total WES score of <6)	11 (10.5)	13 (13.5)	-	0.288†
Optimal wound (total WES score of 6)	94 (89.5)	83 (86.5)	-	0.288†
Wound complication at day 14 using WES [No. (%) of patients]				
Erythema/swelling	1 (1.0)	6 (6.4)	-	-
Infection	1 (1.0)	1 (1.1)	-	-
Minor dehiscence	1 (1.0)	1 (1.1)	-	-
Infection (ASEPSIS: 0-30) [mean±SD]	0.09±0.4	0.61±1.9	-	0.011*
Mean (range) visual analogue scale score for pain				
Baseline (before wound closure)	36.9 (32.0-41.8)	33.6 (29.3-38.0)	3.3 (3.5-9.5)	-
Day 14	10.5 (7.3-13.8)	14.9 (12.0-17.9)	4.4 (0.1-8.8)	-
Month 1	3.6 (1.7-5.4)	8.4 (5.8-11.0)	4.8 (1.7-8.0)	-
Month 3	1.1 (0.3-2.4)	4.1 (2.5-5.7)	3.0 (0.9-5.1)	-
Mean±SD nurse time used (minutes)	20.8±9.1	28.1±8.2	-	<0.005*
Mean±SD wound closure time (minutes)	9±2.4	15±30.9	-	<0.005*
Overall patient satisfaction score (0-100)	91.6	85.3	-	<0.0005*

A difference of 15 in the VACS score was defined as the minimum clinically important between optimal and sub-optimal scar.[14,24] The mean VACS scores at baseline were similar between groups, and the absolute differences at day 14 and months 1 and 3 were not clinically significant (<10), despite the Dermabond group having higher scores (Table 2).

The mean VAS scores for pain at baseline were similar between groups (Fig 3). Repeated measure ANOVA of VAS scores for pain as perceived by participants at the four time points showed no significant main effect for intervention (f (1,198)=2.67, P=0.10, Table 2 and Fig 2). The absolute differences at day 14, months 1 and 3 were all <5 (a minimum difference of 13 was regarded as clinically significant).

Infection score (0-30 scale) at day 14 was significantly lower in the Dermabond group (0.09 vs 0.61, P=0.011, *t* test). As the infection rate was low in both groups, sub-scale analysis revealed that there was a higher rate of erythema/swelling in the suture group (Table 2). The overall patient satisfaction score was higher in the Dermabond group (91.6 vs 85.3, P<0.0005).

The mean time to wound closure was longer in the suture group (9 vs 15, P<0.005), and therefore the mean total nurse time used was also longer (20.8 vs 28.1 minutes, P<0.005). The use of Dermabond could reduce the wound closure time and the nurse time.

Respectively in the Dermabond and suture group, the overall mean costs were HK$241.69 and HK$204.02 (Table 3), and the improvements in mean VACS scores were 30.7 and 23.3. To improve the score on wound appearance by one using Dermabond rather than sutures, an additional HK$5.1 (HK$241.69-204.02/30.7-23.3) was incurred.

Dermabond costs about HK$140 per vial, whereas sutures cost HK$9.5 per package. The higher cost in Dermabond use was mainly due to the equipment cost. Sutures entailed suture removal and more frequent follow-ups for dressing. The substantial cost difference stemmed mainly from the follow-up visits and need to remove stitches (HK$68.5 vs HK$8.2). The suture group drained more nurse services, whereas the Dermabond group incurred a higher equipment cost. Nevertheless, there was no significant difference in costs related to doctors.

Discussion

Cost-effectiveness: hospital administration consideration

The high material cost of the Dermabond could not be offset by its low cost in subsequent wound care. Given the similar clinical outcomes, the conventional suture method appeared to be the preferred method for wound closure from the perspective of hospitals, despite lower infection rate, better wound appearance and patient satisfaction for

Table 3. ost to the Hospital Authority

Variable	Unit cost (HK$)	Dermabond (n=105)			Suture (n=96)		
		No. of patients receiving service	Mean duration of service received (minutes)	Mean cost per person (HK$)	No. of patients receiving service	Mean duration of service received (minutes)	Mean cost per person (HK$)
Costs or wound closure							
Costs or equipment, drugs, and materials							
Normal saline 0.9% or wound dressing	5.2/L	105	-	1.04	96	-	1.04
Local analgesia or sutures (Lignocanie 1%)	2.4/5 mL	4	-	0.13	96	-	2.40
5 ml syringe or infiltration	0.40	4	-	0.02	96	-	0.40
Sterile suture set	3.00	4	-	0.16	96	-	3.00
Simple dressing set	2.70	105	-	2.70	96	-	2.70
Gauze x2 packs	0.36	105	-	0.72	96	-	0.72
Sterile glove	1.70	105	-	1.70	96	-	1.70
Suture material (4'O /5'O) x2 packs	8.25	4	-	0.90	96	-	16.50
Dermabond	140.00	105	-	140.00	0	-	0
Mean±SD subtotal				147.37±5.06			28.46
Absolute difference (95%CI)				118.91 (117.86-119.93)			
Costs or analgesia							
Panadol 500 mg x5 days (20 tabs)	21.0	47	-	10.61	51	-	11.51
Dologesic x5 days (15 tabs)	18.7	9	-	1.81	21	-	4.22
Mean±SD subtotal				12.42±10.17			15.73±8.59
Absolute difference (95%CI)				3.31 (0.59-6.04)			
Costs or human resources*							
Costs or assessment by doctor	5.10	105	5	25.5	96	5	25.50
Costs or wound closure by nurse (procedure)	2.06	105	9	18.41	96	15	30.90
Cost or triage care and advice	2.06	105	12	24.72	96	12	24.72
Costs or reassessment by doctor	5.10	105	1	5.10	96	2	10.20
Mean±SD subtotal				61 ±10.77			78.6 ±12.07
Absolute difference (95%CI)				17.59 (14.75-21.37)			
Mean±SD total costs for wound closure per person				233.52±18.41			135.51±15.54
Absolute difference (95%CI)				98.01 (92.59-102.46)			
Costs or subsequent wound care							
Costs or equipment and materials in suture removal							
Normal saline 0.9% or wound dressing	5.2/L	4	-	0.06	96	-	1.04
Simple dressing set	2.70	4	-	0.15	96	-	2.70
Sterile glove	1.70	4	-	0.09	96	-	1.70
Costs or equipment and materials in wound dressing							
Normal saline 0.9% or wound dressing	5.2/litre	7 (25 visits)	-	0.27	75 (194 visits)	-	2.16
Simple dressing set	2.70	7 (25 visits)	-	0.72	75 (194 visits)	-	5.63
Sterile glove	1.70	7 (25 visits)	-	0.45	75 (194 visits)	-	3.54
Mean±SD subtotal				1.74±7.44			16.77±10.12
Absolute difference (95%CI)				15.03 (12.41-17.55)			
Costs or human resources*							
Costs or suture removal by nurse	2.06	4	8	0.89	93	8	16.48
Costs or wound dressing by nurse	2.06	7 (25 visits)	6	3.32	75 (194 visits)	6	25.65
Costs or subsequent assessment by doctor	5.10	3	5	0.82	3	5	0.82
Costs or subsequent assessment by out-patient doctor	5.10	2	5	0.55	3	5	0.82
Cost or administrative work by clerk	0.87	34 visits	3	0.85	293 visit	3	7.97
Mean±SD subtotal				6.43±22.95			51.74±24.90
Absolute difference (95%CI)				38.19 (31.26-45.12)			
Mean±SD total costs for subsequent wound care per person				8.17±30.20			68.51±34.79
Absolute difference (95%CI)				60.34 (43.74-62.60)			
Mean±SD overall cost to the Hospital Authority per person				241.69±40.92			204.02±39.19
Absolute difference (95%CI)				37.67 (32.76-55.95)			

* Nurse time hourly rate=(mean monthly salary x 12)/(52 x working hours per week)=(HK$23 584 x 12)/(52 x 44); doctor time hourly rate=(mean monthly salary x 12)/(52 x working hours per week)=(HK$58 345 x 12)/(52 x 44); and administrative clerk hourly rate=(mean monthly salary x 12)/(52 x working hours per week)=(HK$10 000x12)/(52 x 44)

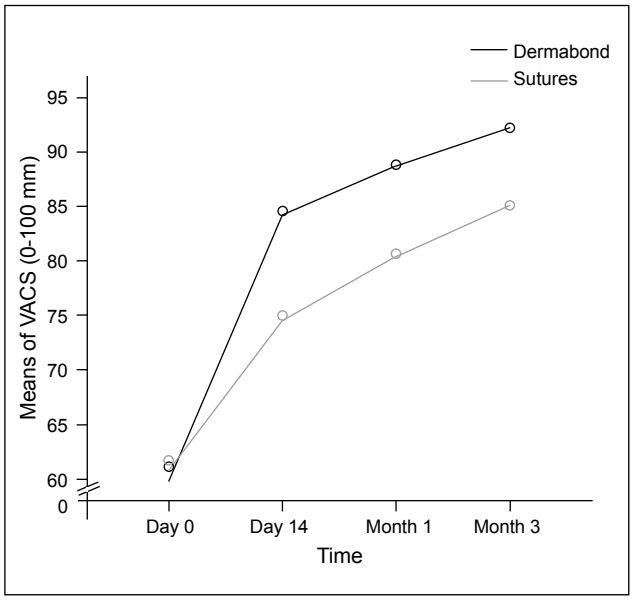

Fig 2. Comparison of visual analogue cosmesis scale (VACS) in Dermabond and suture groups

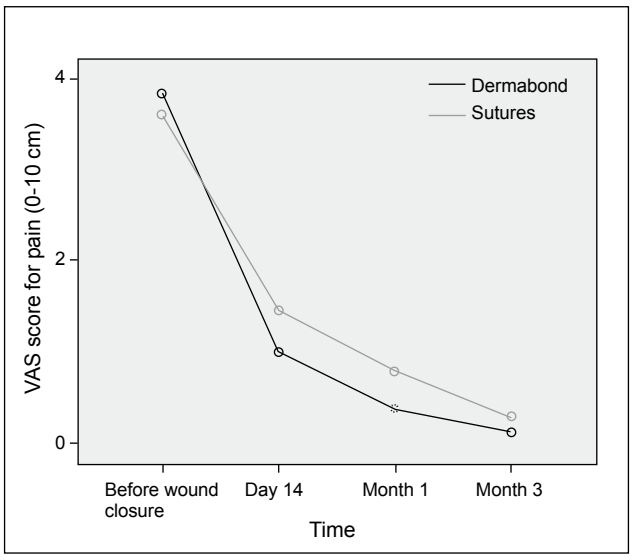

Fig 3. Comparison of visual analogue scale (VAS) score for pain in Dermabond and suture groups

Dermabond.

Cost-effectiveness: patient consideration

The cost-effectiveness analysis did not include charges to patients. Normally each patient needed to pay HK$17 for each dressing, HK$45 for wound reassessment, and HK$100 for each AED attendance. The Dermabond method appeared to be favoured by patients owing to its lower overall charges to them, shorter procedure duration, less frequent follow-up visit, and better patient satisfaction. If a societal viewpoint was taken, which included patient costs and indirect costs such as the value of time taken from work, Dermabond appeared to be more cost-effective and could be adopted more widely and safely in Hong Kong if its supply cost was lower .

Acknowledgement

This study was supported by the Health and Health Services Research Fund (#03040071), Food and Health Bureau, Hong Kong SAR Government. We thank the patients, nursing and medical staff in the accident and emergency departments of the Pamela Youde Nethersole Eastern Hospital and Prince of Wales Hospital for their support in carrying out this study.

References

1. Hospital Authority Intranet. Statistic and research section home site. Retrieved 7 March 2007. Available from http://shis.home/shis/home/default.htm
2. Farion K, Osmond MH, Hartling L, et al. Tissue adhesives for traumatic lacerations in children and adults. Cochrane Database Syst Rev 2002;3:CD003326.
3. Quinn J, Wells G, Sutcliffe T, et al. Tissue adhesive versus suture wound repair at 1 year: randomized clinical trial correlating early, 3-month, and 1-year cosmetic outcome. Ann Emerg Med 1998;32:645-9.
4. Hollander JE, Valentine SM, McCuskey CF, Turque T, Singer AJ. Long-term evaluation of cosmetic appearance of repaired lacerations: validation of telephone assessment. The Stony Brook Wound Registry Study Group. Ann Emerg Med 1998;31:92-8.
5. Bernard L, Doyle J, Friedlander SF, Eichenfield LF, Gibbs NF, Cunningham BB. A prospective comparison of octyl cyanocrylate tissue adhesive (dermabond) and suture for the closure of excisional wounds in children and adolescents. Arch Dermatol 2001;137:1177-80.

Cost implication of team-based structured versus usual care for type 2 diabetic patients with chronic renal disease

GTC Ko 高天才
CY Yeung 楊俊業
WYS Leung 梁潤成
KW Chan 陳健華
CH Chung 鍾振海
LM Fung 馮麗明
TP Ip 葉大鵬
G Kum 甘爾惠
KP Lau 劉錦標
IT Lau 劉業添
JKY Li 李錦燕
SC Siu 蕭成忠
MW Tsang 曾文和
VTF Yeung 楊鐸輝
PCY Tong 唐俊業
WY So 蘇詠儀
JCN Chan 陳重娥

Key Messages

1. Type 2 diabetic patients with chronic kidney disease receiving structured care (SC) by a diabetologist-nurse team or usual care (UC) had a similar incidence of end-stage renal disease (24 of 104 vs 24 of 101) after intervention for 2 years.
2. Patients receiving SC were three times more likely to attain three or more predefined treatment targets than those receiving UC (63 of 104 vs 28 of 101).
3. Of 91 patients who attained three or more treatment targets, 14 died or developed end-stage renal disease, compared to 34 of the remaining 114 patients. This amounted to a 60% risk reduction in favour of SC.
4. The total number of hospital days was 933 in the SC group and 1169 in the UC group, with a cost difference of HK$631 300 over a 2-year period.
5. Using trained nurses to review these patients under medical supervision which incurred an extra cost of HK$476 736 in the SC model was cost-saving in a public health care setting.
6. Assuming all eight extra out-patient visits were medical consultations during the 2-year period, an extra cost of HK$322 172 would have been incurred for the whole group.
7. Using a traditional medical model, additional yearly cost of HK$2557 to 40 272 would be required for a patient to attain multiple treatment targets or save one major clinical event if all review visits were by doctors.

Hong Kong Med J 2011;17(Suppl 6):S9-12

Department of Medicine and Therapeutics, The Chinese University of Hong Kong, Prince of Wales Hospital
GTC Ko, CY Yeung, PCY Tong, WY So, JCN Chan
Queen Elizabeth Hospital
WYS Leung
Princess Margaret Hospital
KW Chan, CH Chung
Caritas Medical Centre
LM Fung
Tung Wah Eastern Diabetes Centre
TP Ip, SC Siu
United Christian Hospital
G Kum, MW Tsang
North District Hospital
KP Lau
Tseung Kwan O Hospital
IT Lau
Yan Chai Hospital
JKY Li
Our Lady of Maryknoll Hospital
VTF Yeung

HSRF project number: S121012

Principal applicant and corresponding author:
Prof Juliana CN Chan
Department of Medicine and Therapeutics, The Chinese University of Hong Kong, The Prince of Wales Hospital, Shatin, Hong Kong SAR, China
Tel: (852) 2632 3138
Fax: (852) 2632 3108
Email: jchan@cuhk.edu.hk

Introduction

Multifaceted care delivered by a multidisciplinary team and attainment of multiple treatment targets are associated with reduced rates of premature mortality and new onset of cardiovascular disease in type 2 diabetes.[1,2] In a quality improvement programme involving type 2 diabetic patients with chronic kidney disease, those managed by a pharmacist-diabetologist team using a structured care (SC) protocol were more likely to attain multiple treatment goals and had 50% lower risk of death or end-stage renal disease than those treated with usual care (UC).[3]

Patients and methods

In a 2-year multicentre study conducted between 2004 and 2007,[4] 205 type 2 diabetic patients aged 35 to 75 years from nine public hospitals were randomised to receive either SC delivered by a diabetes specialist team using a protocol with predefined treatment targets or UC. Their serum creatinine levels were 150 to 350 μmol/L. None had biopsy proven glomerulonephritis or surgically remediable renal disease. The primary renal endpoint was defined as death and/or end-stage renal disease (need for dialysis or plasma creatinine level of ≥500 μmol/L). The composite cardiovascular endpoint consisted of acute myocardial infarction, lower extremity amputation, revascularisation procedures, heart failure, unstable angina, and arrhythmia precipitating hospital admission. The study protocol was approved by the ethics review committee of the participating hospitals.

The treatment targets were defined as blood pressure of <130/80 mm Hg, HbA_{1c} of <7%, LDL-C of <2.6 mmol/L, triglyceride of <2 mmol/L, and treatment with angiotensin-converting enzyme inhibitors and/or angiotensin II receptor blocker provided that the patients did not develop persistent hyperkalaemia (≥5.5 mmol/L) or acute deterioration in plasma creatinine (eg 30% increase) upon introduction or dose titration of these drugs.

Patients randomised into the SC group were seen by a dietician to reinforce adherence to a low protein and low potassium diet. Patients were first started on either an angiotensin-converting enzyme inhibitor or an angiotensin II receptor blocker, and their renal function was monitored at week 2, and then 4-weekly for 12 weeks, and every 8 to 12 weeks thereafter. All patients were seen at the diabetes centre by a diabetologist (or endocrine trainee) and a diabetes nurse at least four times each year, and more often if indicated. Between each medical review, patients were followed up by the diabetes nurse for blood taking, measurement of body weight and blood pressure, and reinforcement of self-care and treatment compliance. All laboratory results were available for medical review at the next visit for decision making.

Patients randomised into the UC group were managed according to the usual practice of the participating hospitals. Thus, patients might attend a diabetes clinic or a general medical clinic, usually at 3 to 4 monthly intervals. All clinical decisions or referrals for investigations or education were at the doctor's discretion.

Results

The results of this study have been reported.[4] In brief, 24 of the 104 patients receiving SC and 24 of the 101 patients receiving UC reached the primary renal endpoint. After adjusting for age, gender, and study sites, the SC group had lower diastolic blood pressure (68±12 vs 71±12 mm Hg, P=0.02) and HbA_{1c} levels (7.3±1.3% vs 8.0±1.6%, P<0.01) and was more likely to attain three or more treatment goals (61% [63/104] vs 28% [28/101]). Patients who attained three or more treatment goals (n=91) had 60% risk reduction in reaching the primary renal endpoint than those who did not (n=114) [14 vs 34; RR=0.43; 95% confidence interval, 0.21-0.86].

The clinical events and hospitalisation days in patients randomised to SC or UC group are summarised (Fig 1). Using Kaplan-Meier plots, the time to first clinical event (including death, renal and cardiovascular endpoints) is shown (Fig 2). The cost estimates for the SC and UC groups are shown (Table). The total number of hospital days during the 2-year study period was 933 in the SC group and 1169 in the UC group, with a difference in hospitalisation costs of HK$631 300 (US$80 935). In the SC group, 35 more patients attained multiple treatment targets, and there were four fewer composite renal endpoints and six fewer combined clinical endpoints than in the UC group. In a traditional medical model, each patient in the SC group would need eight extra medical consultations during the 2-year period incurring an extra cost of HK$322 172 (US$41 410) after deducting savings from hospitalisation costs. Based on these estimates, an additional yearly cost of HK$2557 to 40 272 (US$329 to 5176) would be required for a patient to attain multiple treatment targets or save one major clinical event. In this team-based model, we used trained nurses to review these patients which was cost-saving in a public health care setting, even if we factored medical input (eg 20% of a medical clinic visit) into the calculation.

Discussion

In this multicentre, randomised translational study, although we failed to show that SC was more effective than UC in reducing the renal endpoint, three times more patients in the SC group attained multiple treatment targets compared to the UC group. Patients who attained multiple treatment targets had 60% risk reduction in death and end-stage renal disease.[4] When the study was first conceived in 2000, the sample size was estimated using data available at that time.[3,5] In earlier studies conducted between 1997 and 2002 which recruited patients with similar characteristics, the incidence of the primary renal endpoint was 30 to 50% over a 2-year period. In the present study, a rate of 24% was noted for the primary renal endpoint in both the SC and UC groups. This suggests that increasing awareness of the beneficial effects of intensive risk factor control and inhibition of the renin-angiotensin system had led to improvement in care standard

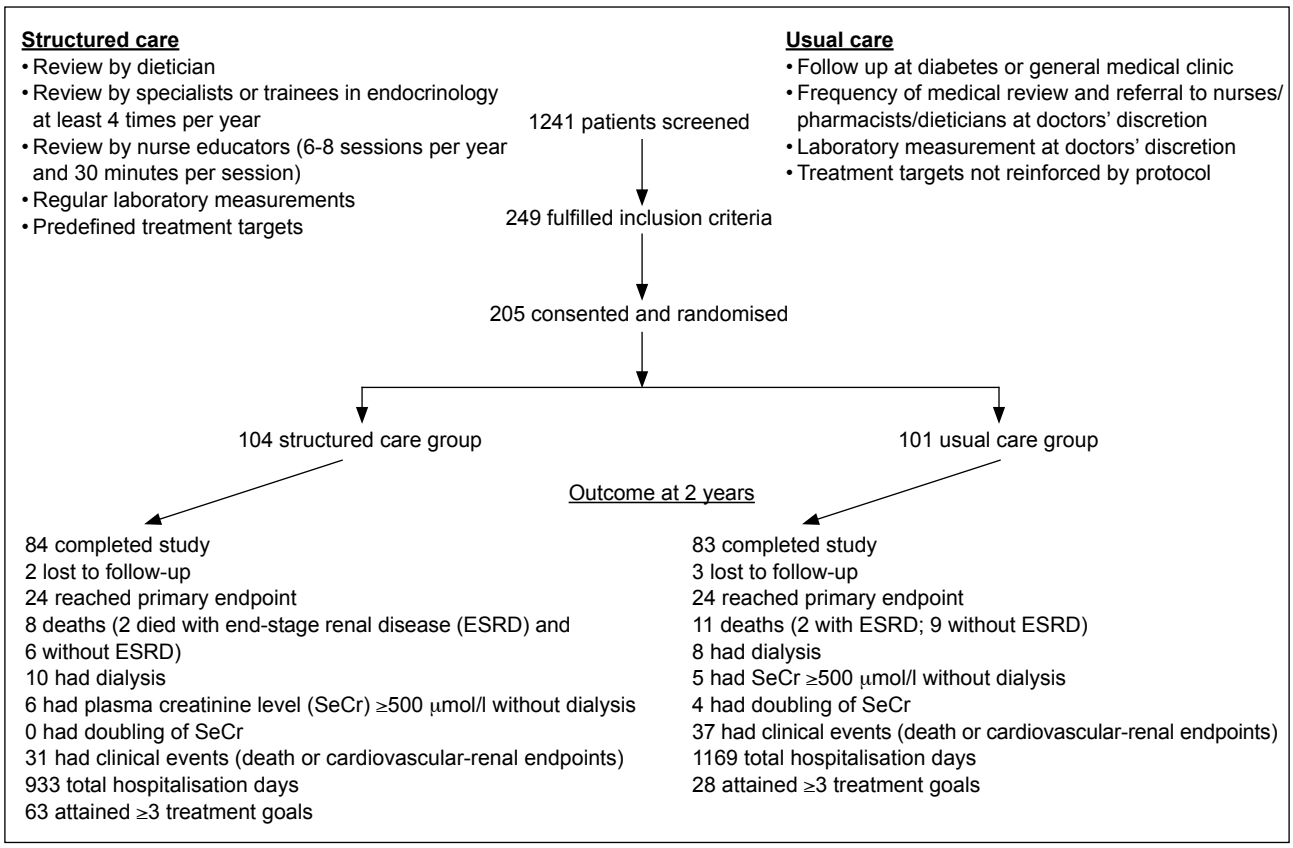

Fig 1. Recruitment, randomisation, and clinical outcomes of type 2 diabetic patients with chronic kidney disease

and reduced rates of clinical endpoints. The involvement of specialist care in the UC group in some of the hospitals might have reduced the effect size of SC. Furthermore, the lack of an audit to reinforce adherence to protocols and attainment of multiple treatment targets in the SC group might also explain the apparent failure to benefit in the SC group.[4]

The three-fold higher rate for attaining multiple treatment targets in the SC group translated to a lower mortality rate, fewer clinical events and hospitalisation days, which are all in agreement with other studies.[1,2] In an observational study of 6386 type 2 diabetic patients, attainment of two or more treatment targets was associated with 30 to 50% risk reduction in new onset of cardiovascular disease.[2] In the Steno-2 study, patients receiving multifaceted care were more likely to attain multiple treatment targets than those receiving usual care. This translated to 20 to 60% risk reduction in death, microvascular, and macrovascular complications.[1]

From a public hospital perspective, the additional costs incurred in the SC group were mainly due to extra clinic visits, laboratory tests, and drug costs. Taking into consideration of lower hospitalisation costs in the SC group, we estimated an additional yearly cost of HK$2557 to HK$40 272 (US$328 to 5176) would have been needed to treat one patient to attain multiple treatment targets or save one clinical event if only doctors were used to manage these high-risk patients. In this team-based model, our patients were reviewed by trained nurses (supervised by a specialist) in the SC model which became cost-saving. In the United Kingdom Prospective Diabetes Study, the cost per quality-adjusted life year (QALY) for intensive blood glucose control with insulin or sulfonylureas was £6028 higher than for conventional treatment, whereas that with metformin in overweight patients was £1856 less than conventional treatment. The cost per QALY gained for tight blood pressure control was £369.[6] According to the Centers for Disease Control in the USA, the incremental cost:effectiveness ratio for intensive glycemic control was US$41 384 per QALY. On the other hand, intensified blood pressure control and reduction of serum cholesterol were cost-saving with US$1959 and US$51 889 gained per QALY, respectively. These interventions were most cost-effective when instituted early during the course of disease.[7] In the Steno-2 Study, the incremental cost:effectiveness ratio for multifaceted care versus conventional treatment was €3927 and €2538 per life year and per QALY gained, respectively. These incremental costs were mainly attributed to increased pharmacy and consultation costs.[8]

There are multiple barriers in delivering SC at the levels of patients, care providers, and health care systems. In most clinical audits, <10% of type 2 diabetic patients attained three or more treatment targets (namely blood pressure, LDL-C, and HbA_{1c}).[9] Apart from patient noncompliance, clinical inertia of physicians with delayed commencement

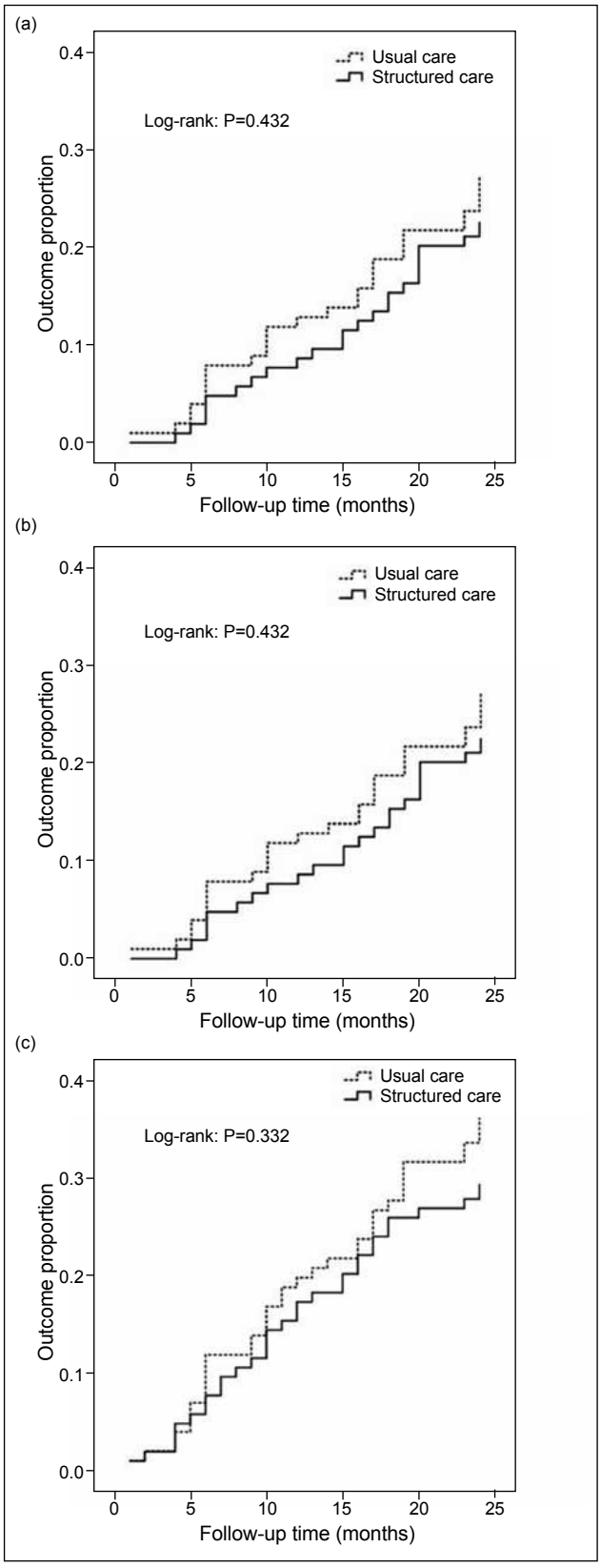

Fig 2. Kaplan-Meier plots showing the cumulative incidences of the (a) primary renal endpoint, (b) composite renal endpoint, and (c) combined endpoint during a 2-year period

Primary renal endpoint is defined as death or need for dialysis or serum creatinine level of ≥500 μmol/L; composite renal endpoint is defined as primary renal endpoint or doubling of the serum creatinine level; and combined endpoint is defined as composite renal or cardiovascular endpoints

Table. Comparison of treatment costs between the structured care (SC) and usual care (UC) groups during a 2-year period

Cost (HK$)	SC (n=104)	UC (n=101)
Treatment costs		
No. of clinic review by doctors per year per patient	4	4
Extra No. of clinic review by nurses per year per patient	4	
Cost of each clinic review by doctors (Hospital Authority statistical report, 2004-5)	1146	1146
Cost of each clinic review by nurses (estimated 50% of above)	573	-
Additional costs		
Extra cost of nurse review per patient (573×4 visits×2 years)	4584	
Total extra cost of nurse visits in 2 years (4584×104 patients)	476 736	
Assuming all additional visits are medical consultations (1146×8 visits×104 patients)	953 472	-
Hospitalisation costs		
Mean/median (IQR) days of hospitalisation per patient	8.97/2 (0-10)	11.57/2 (0-15)
Total days of hospitalisation of the whole arm	933	1169
Cost per hospitalisation day (Hospital Authority statistical report 2004-5)	2675	2675
Total cost spent on hospitalisation	2 495 775	3 127 075
Cost saving in SC group (if extra visits by nurses)	-154 564	-
Extra cost in SC group (if extra visits by doctors)*	322 172	-
Clinical outcome		
No. of patients attaining ≥3 treatment targets	63	28
No. of patients reaching composite renal endpoint (death+need for dialysis+doubling of serum creatinine level)	24	28
No. of patients reaching combined endpoint (death+cardiovascular-renal endpoint)	31	37

* During a 2-year period, extra cost needed to (1) treat one patient to attain multiple treatment targets (35 more patients in SC group): HK$322 172÷35=5114, (2) prevent one composite renal endpoint (four fewer endpoints in SC group): HK$322 172÷4=80 543, and (3) prevent one combined endpoint (six fewer endpoints in SC group): HK$322 172÷6=53 695

or escalation of therapy might also reduce the likelihood of achieving multiple treatment targets.[10] To this end, our results strongly support the cost-effective nature of using a doctor-nurse team to implement structured care. Increasing the sample size, lengthening the follow-up period and introducing an audit system to improve protocol compliance and attainment of multiple treatment targets will be necessary to confirm these encouraging findings.

Conclusions

In this 2-year study, although type 2 diabetic patients treated with SC had a similar incidence of death or end-stage renal disease as those treated with UC, they were more likely to attain multiple treatment targets and had reduced hospitalisation rates. Given the silent nature of diabetes and the complex nature of care protocols, an integrated and team-based approach (including early diagnosis, risk stratification, use of protocol with predefined targets and management plans, and decision support) further augmented by regular feedback and patient empowerment is needed to achieve favourable outcomes.

Acknowledgements

This study was supported by the Health Services Research Fund (#s121012), Food and Health Bureau, Hong Kong SAR Government. We thank our research nurses—Ms Germaine Cheung and Ms Yee Mui Lee—for their assistance in coordinating the project and entering all data. We also thank the following diabetes nurses for their dedication in managing the patients: E Kan (Alice Ho Miu Ling Nethersole Hospital), MT Chan (Caritas Medical Centre), LH Lin, ML Tong (North District Hospital), JJ Kwan, H Tang, YC Han (Our Lady of Maryknoll Hospital), CS Law (Tseung Kwan O Hospital), C Wong (Tung Wah Eastern Hospital), PH Mok (United Christian Hospital), A Leung (Yan Chai Hospital), and M Siu (Princess Margaret Hospital).

References

1. Gaede P, Lund-Andersen H, Parving HH, Pedersen O. Effect of a multifactorial intervention on mortality in type 2 diabetes. N Engl J Med 2008;358:580-91.
2. Kong AP, Yang X, Ko GT, et al. Effects of treatment targets on subsequent cardiovascular events in Chinese patients with type 2 diabetes. Diabetes Care 2007;30:953-9.
3. Leung WY, So WY, Tong PC, Chan NN, Chan JC. Effects of structured care by a pharmacist-diabetes specialist team in patients with type 2 diabetic nephropathy. Am J Med 2005;118:1414.
4. Chan JC, So WY, Yeung CY, et al. Effects of structured versus usual care on renal endpoint in type 2 diabetes: the SURE study: a randomized multicentre translational study. Diabetes Care 2009;32:977-82.
5. Chan JC, Wat NM, So WY, et al. Renin angiotensin aldosterone system blockade and renal disease in patients with type 2 diabetes. An Asian perspective from the RENAAL Study. Diabetes Care 2004;27:874-9.
6. Gray AM, Clarke P. The economic analyses of the UK prospective diabetes study. Diabet Med 2008;25(Suppl 2):S47-51.
7. CDC Diabetes Cost-effectiveness Group. Cost-effectiveness of intensive glycemic control, intensified hypertension control, and serum cholesterol level reduction for type 2 diabetes. JAMA 2002;287:2542-51.
8. Gaede P, Valentine WJ, Palmer AJ, et al. Cost-effectiveness of intensified versus conventional multifactorial intervention in type 2 diabetes: results and projections from the Steno-2 study. Diabetes Care 2008;31:1510-5.
9. Chan JC, Gagliardino JJ, Baik SH, et al. Multifaceted determinants for achieving glycemic control: the International Diabetes Management Practice Study (IDMPS). Diabetes Care 2009;32:227-33.
10. So WY, Chan JC. The role of the multidisciplinary team. In: Textbook of diabetes. 4th ed. Holt R, Cockram S, Flyvbjerg A, Goldstein B,, editors. Blackwell; 2010:969-83.

R Fielding 莊日昶
GCF Chan 陳志峰
WWT Lam 藍詠德

Health-related quality of life assessment for Hong Kong Chinese children with cancere

Key Messages

1. The direct measurement of quality of life in young children aged 30 to 72 months is feasible and valid.
2. An interactive storybook was developed to help inform young children with cancer of the medical procedures and consequences. The storybook had good construct, convergent, and criterion validity.

Introduction

Evaluation of health-related quality of life (QoL) in young children aged <5 years with cancer relies on proxy assessments by nurses or parents.[1-5] Both of which are subject to bias known as cross-informant variance.[6] Most children over 3 years old have the capacity to respond in a meaningful and reliable way, provided that they are assessed in an age-appropriate manner.[7] This would enable direct assessment of QoL in children. We therefore (1) developed an age-appropriate direct assessment of QoL for children aged 3 to 5 years with cancer, and (2) validated its use in children of southern Chinese cultural background aged 5 to 8 years, using an established QoL module specifically for cancer-related problems—the PedsQLCa.[8]

Methods

This study was conducted from January 2005 to December 2006. The development of the QoL assessment for children aged 3 to 5 years was based on an interactive 16-page storybook depicting the experiences of a gender-neutral cartoon bear going through a range of medical procedures and consequences typical to children having cancer. The child was asked to give two responses to each question on a 'smiley scale' and on an 'intensity thermometer', which broadly assess quality and intensity of the experience associated with the depicted scenarios. The storybook was developed over a 12-month period, and included detailed scrutiny and restructuring of each page's content. It took note of the ability of children to sustain the necessary attention and the ability of 3 to 5 years old to reliably link feeling states to several potential response formats, which were piloted and reviewed to produce the finalised storybook. On each page, one or more questions were asked regarding the experience depicted in each scenario, and up to two scores per question were produced: a five-point categorical scale indicating quality of experience (very good to very bad) and a three-point measurement of intensity (a little, somewhat, very much).

This instrument was then administered to newly recruited children in the target group (30 to 72 months old, with a diagnosis of cancer) attending one of five hospitals in Hong Kong and Shenzhen. Scores for all 26 questions were recorded on a pre-designed score sheet. Caretakers completed the PedsQLCa, whereas nurses concurrently completed both the PedsQLCa and several seven- and 10-point categorical scales measuring fatigue, pain (acute and chronic), general wellness, and eating. Clinical and sociodemographic data were also collected.

To validate the PedsQLCa, 135 children aged 60 to 108 months were recruited from five regional hospitals in the Pearl River Estuary region of southern China. A standard ethnographic translation-back-translation procedure was used to produce the Chinese version of the PedsQLCa. Eligible children completed the PedsQLCa after they and their parent/caretaker gave informed consent.

For analysis of PedsQLCa, individual scores for each page were recorded on a page-by-page basis and entered into a computer. The PedsQLCa produces separate module scores by summing scores for the eight modules (pain, nausea,

Hong Kong Med J 2011;17(Suppl 6):S13-6

The University of Hong Kong: Centre for Psycho-oncology Research & Training, Behavioural Sciences Unit
R Fielding, WWT Lam
Department of Paediatrics & Adolescent Medicine
GCF Chan

HHSRF project number: 02030161

Principal applicant and corresponding author:
Prof Godfrey CF Chan
Department of Paediatrics & Adolescent Medicine, The University of Hong Kong, Pokfulam, Hong Kong SAR, China
Tel: (852) 2855 4091
Fax: (852) 2855 1523
Email: gcfchan@hkucc.hku.hk

treatment anxiety, worry, cognitive problems perceived physical appearance, and communication). The PedsQLCa avoids the problems of scaling by having no total score but just factor scores. Nonetheless, this makes the use of factor analysis inappropriate.

Correlations between concurrent nurse and caretaker assessments were calculated to determine the degree of observer concordance. Module scores by different assessors (caretaker vs nurse) were compared, and differences in children on and off active chemotherapy cycles to determine criterion validity were examined using the known groups approach.

For analysis of the storybook, higher scores indicate better QoL status. All scores were transformed to a range of 0 to 100. Two sets of data (feeling scores for different experiences [happy/unhappy]; intensity scores of pain, discomfort, nausea, alopecia, mucositis) were analysed separately. Each was subject to separate principal component analysis using oblique rotation. Factor and total scores were then calculated and correlated with caretaker and nurse PedsQLCa scores to determine convergent validity.

For the sub-set of children for whom both storybook and PedsQLCa assessments were available, correlations were performed to determine convergent validity. Responses completed in children who received active treatment within the past month were compared to those in children who had been treatment-free for at least 3 months to determine clinical (criterion) validity. Comparisons between children with cancer and those with thalassaemia were made to further examine clinical validity. Responses within children who, on both assessments, had been in remission for more than 3 months were used to assess test-retest reliability.

Results

Instrument content

The storybook was compiled to match the aspects of the PedsQLCa in terms of the domains covered and then evolved to fit local clinical scenarios. The draft instrument comprised 16 pages, involving 25 questions, each addressing different aspects of the cancer experience. For each item, the first digit refers to the page, the second to the item number (up to five) on that page. These included anticipatory anxiety about hospital attendance (item 1.1) and medical procedures (item 1.2), feelings about going to the hospital (item 2), feelings when waiting for the consultation (item 3), feelings during the consultation (item 4), separation anxiety (item 5), anticipatory anxiety regarding blood draw (item 6), feeling and intensity of blood drawing (item 7), central venous line experience (item 8), lumbar puncture (item 9), anticipatory anxiety about medication (item 10), fever following medication (item 11.1), oral soreness (mucositis) following medication (item 11.2), nausea after medication (item 11.3), hair-loss after taking medication (item 11.4), nausea when presented with food (item 12, if yes then), nausea on smelling food (item 12.1), nausea-related food refusal (item 12.2), and lack of appetite (item 12.3), fever after chemotherapy (item 13.1), oral mucositis after chemotherapy (item 13.2), nausea after chemotherapy (item 13.3), hair loss after chemotherapy (item 13.4), fatigue after chemotherapy (item 13.5), activity level at home (item 14), post-treatment hair loss (item 15), embarrassment if any scarring is viewed (item 16).

Assessments

A total of 161 assessments (at different time points) were completed by children using the storybook for which there were concurrent caretaker assessments; 294 assessments

Table 1. Five-factor solution of observed variance following principal component analysis

Item	Factor 1	Factor 2	Factor 3	Factor 4	Factor 5
7: Experience of blood drawing	0.766	-	-	-	-
9: Lumbar puncture	0.739	-	-	-	-
6: Anticipatory anxiety about blood drawing	0.738	-	-	-	-
8: Central venous line experience	0.556	-	-	-	-
5: Separation anxiety	0.475	-	-	-	-
10: Anticipation about medication	0.467	-	-	-	-
14: Hair loss after medication/chemotherapy	-	0.807	-	-	-
13.3: Nausea after medication/chemotherapy	-	0.795	-	-	-
13.5: Fatigue after medication/chemotherapy	-	0.669	-	-	-
13.2: Oral mucositis after medication/chemotherapy	-	0.606	-	-	-
12: Nausea on presentation of food	-	0.584	-	-	-
12.1: Nausea on smell of food	-	-	0.886	-	-
12.2: Nausea-related food refusal	-	-	0.815	-	-
12.3: Lack of appetite	-	-	0.809	-	-
4: Feelings during consultation	-	-	-	0.769	-
3: Waiting for consultation	-	-	-	0.674	-
1.1: Hospital attendance	-	-	-	0.543	-
16: Embarrassment over scars	-	-	-	0.494	-
1.2: Anticipation of medical procedures	-	-	-	0.492	-
2: Feelings about going to hospital	-	-	-	-	0.682
13.1: Fever after chemotherapy	-	-	-	-	0.669
14: Activity level at home	-	-	-	-	0.572

Table . Three-factor solution of intensity items following principal component analysis

Item	Factor 1	Factor 2	Factor 3
13.3.2: Intensity of nausea after medication/chemotherapy	0.795	-	-
13.4.2: Intensity of hair loss after chemotherapy	0.787	-	-
13.1.2: Intensity of fever after chemotherapy	0.733	-	-
13.2.2: Intensity of discomfort from mucositis after chemotherapy	0.724	-	-
13.5.2: Intensity of fatigue after chemotherapy	0.561	-	-
12.2.2: Intensity of food-related nausea/refusal after chemotherapy	-	0.939	-
12.1.1: Intensity of food smell–induced nausea	-	0.908	-
12.3.2: Intensity of appetite loss after chemotherapy	-	0.779	-
9.2: Intensity of discomfort about lumbar puncture	-	-	0.807
7.2: Intensity of discomfort about blood drawing	-	-	0.805
8.2: Intensity of discomfort about central venous line	-	-	0.754

were completed by children using the PedsQLCa, 187 of which also had concurrent caretaker assessments, whereas 48 assessments were completed by children using both assessments for which there were concurrent caretaker assessments. Only 30 nurse assessments were completed despite repeated efforts to improve the response rate.

The storybook generates two dimensions of responses: feelings (positive or negative, in a five-point scale) and intensity of feeling (mild, medium, severe in a three-point scale). These two sets of dimensions were treated independently in the first instance in order to determine if the factor structure of the instrument was both coherent and approximated to the PedsQL factor structure.

The five-factor solution accounted for 55.25% of the observed variance (Table 1). The five factors were: procedural and separation anxiety (procedures) [6 items, 17.68% of variance], symptoms (symptoms) [5 items, 12.15%], nausea (3 items, 11.34%), treatment anxiety (treatment) [5 items, 7.37%], and at home (home) [3 items, 6.71%]. The 11 intensity items were subject to obliquely rotated principal component analysis which yielded a Kaiser-Meyer-Olkin measure of 0.629 and a significant Bartlett's test score. A three-factor solution accounted for 64.9% of the observed variance. The three factors were symptom intensity (5 items, 26.39%), nausea intensity (3 items, 20.75%), and invasive procedure intensity (3 items, 17.78%) [Table 2].

Discussion

Treatment decision making difficulties and outcome expectancies strongly predicted postoperative and outcome psychological morbidity after adjustment for disposition and coping efficacy, consultations, mediated by treatment decision making–related factors can exacerbate baseline distress, in turn mediating adjustment one month postoperatively.

Physical symptom distress, accounting for most variance in outcome CHQ12, was itself predicted by active treatment and baseline CHQ12.

Table 3. Factor structure (pattern matrix) of storybook

Factor structure	Active treatment (scores)		P value
	On (n=10)	Off (n=61)	
Procedural and separation anxiety	51.10	54.66	>0.05
Symptoms	13.48	19.65	>0.05
Nausea	20.23	2.80	0.004
Treatment anxiety	29.74	40.40	>0.05
Home	31.92	40.23	>0.05
Symptom intensity	87.5	78.06	>0.05
Nausea intensity	80.83	96.94	0.011
Procedure intensity	79.17	55.47	0.042

Chemotherapy paradoxically enhanced physical symptom distress, but lowered follow-up psychological morbidity. Chinese women may feel that they are receiving additional treatment thereby gaining reassurance from chemotherapy while experiencing the side-effects.[1,7] So symptoms are worse, but worry is less. We did not find similar reports on western patients.

Comparisons between storybook and PedsQLCa

A subset of 30 children aged 60 to 71 months completed both the storybook and the PedsQLCa. Correlations (*r*) were moderate (range, <0.01-0.10) for conceptually unrelated items and up to 0.357 for more strongly related items. Associations showed conceptual (nausea: nausea; anxiety-anxiety) correspondence and consistency (both feeling and intensity scores loaded on the same PedsQLCa module). Factor 4 (treatment anxiety) in particular correlated with a number of dimensions including worry, appearance, communications, treatment, and procedural anxiety, whereas procedural/separation anxiety correlated with PedsQLCa pain, treatment anxiety, and perceived appearance. Storybook nausea correlated with PedsQLCa nausea, cognitive difficulties, and perceived appearance, whereas storybook procedural intensity correlated with PedsQLCa pain, procedural anxiety, worry, perceived appearance, and cognitive difficulties.

Comparisons between child-completed storybook and proxy caretaker- and nurse-completed PedsQLCa

We examined if the child-completed storybook scores

corresponded more closely with those of the caretaker proxy scores on the PedsQLCa for younger children (under 72 months of age). These correlations showed similar patterns, but were weaker than those in children who self-completed both instruments. Correspondence was greatest for nausea and least for anxiety and procedural intensity.

Discriminant/criterion validity (known groups approach)

To explore if the storybook were able to discriminate between children who had higher or lower QoL, we compared scores in children who were on and off active treatment. Storybook scores in nausea feeling, symptom intensity, and procedural intensity were differentiated between the two groups (Table 3). All other scores indicated better QoL among the off-treatment group.

Conclusion

The storybook had a valid factor structure within its two key dimensions of feeling and intensity, suggestive of good construct validity, whereas the correlations with the PedsQLCa indicated good convergent validity. All factor scores, particularly both feeling and intensity nausea factors, significantly differentiated between children on and off treatment, suggesting that the instrument had effective criterion validity. Further development in this area is warranted.

Acknowledgements

This study was supported by the Health and Health Services Research Fund (#02030161), Food and Health Bureau, Hong Kong SAR Government. We thank Queen Mary Hospital, Queen Elisabeth Hospital, Princess Margaret Hospital, Tuen Mun Hospital, Shenzhen Children Hospital, and Nanfang Hospital for their support.

References

1. Goodwin DA, Boggs SR, Graham-Pole J. Development and validation of the Paediatric Oncology Quality of Life Scales. Psychol Assess 1994;6:321-8.
2. Lansky SB, List MA, Lansky LL, Ritter-Sterr C, Miller DR. The measurement of performance in childhood cancer patients. Cancer 1987;60:1651-6.
3. Trudel JG, Rivard M, Dobkin PL, Leclerc JM, Robaey P. Psychometric properties of the Health Utilities Index Mark 2 system in paediatric oncology patients. Qual Life Res 1998;7:421-32.
4. Yeh CH, Hung LC. Construct validity of a newly developed quality of life assessment instrument for child and adolescent cancer patients in Taiwan. Psychooncology 2003;12:345-56.
5. Collins JJ, Byrnes ME, Dunkel IJ, et al. The measurement of symptoms in children with cancer. J Pain Symptom Manage 2000;19:363-77.
6. Varni JW, Katz ER, Colegrove R Jr, Dolgin M. Adjustment of children with newly diagnosed cancer: cross-informant variance. J Psychosoc Oncol 1995;13:230-8.
7. Eiser C. Quality of life in children with cancer. Proceedings of the British Psychological Society, 11, 1 February 2003, p13.
8. Varni JW, Burwinkle TM, Katz ER, Meeske K, Dickinson P. The PedsQL in pediatric cancer: reliability and validity of the Paediatric Quality of Life Inventory Generic Core Scales, Multidimensional Fatigue Scale, and Cancer Module. Cancer 2002;94:2090-106.

SM McGhee 麥潔儀
J Brazier
CLK Lam 林露娟
LC Wong 黃麗君
J Chau 周宗欣
A Cheung 張惠棱
A Ho 何麗儀

Quality-adjusted life years: population-specific measurement of the quality componente

Key Message

A valid scoring algorithm was developed to translate local SF-36 datasets to quality-adjusted life years.

Introduction

The ever-increasing demand on health care services results in a growing demand for appropriate methods of measuring and valuing the benefits of health care interventions (cost-effectiveness) in order to formulate policies. In Hong Kong, there is little explicit information to guide policymaking on which treatments to offer and what priority to allocate to differing sectors of the health care system.

A principal approach for incorporating preferences into a measure of health has been to value health status in a single unit of measurement known as quality-adjusted life years (QALYs),[1] which combines increased life expectancy and improvements in health status. This assigns to each period of time a 'quality weight' ranging from 0 to 1, which corresponds to the health-related quality during that period, where a weight of 1 is given to optimal health, and 0 to a health state equivalent to death. The number of QALYs is the value given to each state multiplied by the length of time spent in that state; thus a person expected to survive 10 years at a mean quality of 0.8 has 8 QALYs.

The Short Form-36 (SF-36) is a measure of perceived health status evolved out of two major research programmes in the USA.[2,3] It has become one of the most widely used measures of health status in clinical trials throughout the world. The SF-36, and its shorter version, the SF-12, have been assessed for relevance, translated and validated in Hong Kong.[4-9] This local version (SF-36 HK) is also widely used. In the United Kingdom, valuation data were collected, and a model was estimated to allow the calculation of a preference-based index for the English version of the SF-36 in its population.[10] Nonetheless, there is a major scientific concern when using UK preference weights in other countries.

We aimed to derive an algorithm to translate SF-36 data to utility weights for use in Hong Kong. The objectives were (1) to use a representative sample of the local population to obtain a series of valuations of health states that are locally relevant, based on the Hong Kong Chinese version of the SF-36 (SF-36 HK); (2) to use these valuations to derive a model which can be used to predict the value of any health state described by the SF-36 HK; and (3) to compare the final model results with the model already derived for the UK population to identify any systematic differences in valuations.

Methods

This study was conducted from 30 September 2004 to 30 June 2006. We valued a small number of health states, which could be extrapolated to all health states described by the SF-36. These health states were described by the SF-6D, a subset of the SF-36. The first step in creating the Hong Kong-based utility weights was to develop the SF-6D HK.

The SF-6D asks about six aspects of health (physical functioning, role limitations, social functioning, pain, mental health, and vitality) over the past 4 weeks. A health state is defined by taking one level from each of the six different aspects of the SF-6D, so each health state is described by six digits. The Chinese Hong Kong version of the SF-6D was derived from the English UK version by

Hong Kong Med J 2011;17(Suppl 6):S17-21

The University of Hong Kong: School of Public Health
SM McGhee, LC Wong, J Chau, A Cheung, A Ho
Department of Family Medicine and Primary Care
CLK Lam
University of Sheffield, United Kingdom
J Brazier

HHSRF project number: 02030351

Principal applicant and corresponding author:
Prof SM McGhee
School of Public Health, The University of Hong Kong, Pokfulam, Hong Kong SAR, China
Tel: (852) 2819 9280
Fax: (852) 2855 9528
Email: smmcghee@hku.hk

forward-backward translations. The SF-6D HK was field-tested in a pilot study and showed that the valuation method was feasible and the resulting data were reliable and fitted quite well in an econometric model.[11]

A representative sample was obtained through a random digit telephone survey between 17 October 2004 and 23 December 2005. Cantonese speaking residents aged ≥18 years were included. When a household was identified, a Kish Grid method was used to target a random respondent from a list of household members ranked by age. That person was asked for, and if unavailable an arrangement was made to call him/her back at a more convenient time. When the target respondent was contacted, some initial data (SF-6D, age, sex, educational level, living district, smoking status) were collected. An arrangement was made for a face-to-face interview to carry out the standard gamble procedure. To encourage participation, the face-to-face interviews were held in local community halls at convenient times of the day and evening, including weekends. A letter stating the date, time, and location of the interview was sent to each respondent 2 weeks earlier, and a reminder call was made the night before. Any respondent who did not show up was called for. Those who participated were given HK$100 for travelling expenses.

The composition of the final sample of face-to-face interviews was monitored with regard to sex, age, and district of residence. In the later stage of recruitment, there were insufficient respondents in the youngest age group (18 to 39 years). Therefore, recruitment of this group continued while recruitment of the other age groups had ceased.

Selection and valuation of health states

There were 196 health states selected as being able to be extrapolated to the full set of 18 000 states described by the SF-36. Each respondent was asked to value seven health states in a random order. In order to ensure each person valued a range of health states from very mild to very severe, the states were stratified into a block system.

The interview procedure was modelled on that used in the UK study, which was based on methodology developed at McMaster University, Canada. Each participant was asked to rank a set of ten health state cards and then rate them using a visual analogue scale of 0 to 100 points, where the endpoints were the best and the worst imaginable health states. This ranking and rating exercise was followed by the standard gamble procedure. While evaluating each of the seven health states, the participants were asked to choose between an intervention (choice A) involving uncertain health outcomes and a certain health state defined by the SF-6D HK states (choice B). There were two possible health outcomes in choice A: the best health state (H) if the treatment was successful and the worst health state (K) if the treatment failed. The seven health states were placed in choice B one by one as the certain health state under valuation. Once the seven states had been valued, an eighth choice was presented. The reference state in choice A was represented by the state judged by this individual as the poorest, either K or L. The other one of states K or L then became choice B. This enabled valuation of K against L.

Choice A, the intervention, involved the best health outcome with probability P and the worst health outcome with probability $1–P$. The probability of the outcomes was varied until the respondent was indifferent between choosing A or B. At that point, the preference-based utility value of the health state in choice B was reached. The respondent was asked for further information on marital status, number of children, employment, place of birth, number of family members, type of housing, household income, medical benefits, and health-related questions in order to control for these in the analysis. The value for each health state was then transformed to a scale with 1 as full health and 0 equivalent to death.

The modelling methods used were the same as for the UK study.[12] Two main modelling approaches were used with either individual level data, which takes into account the variation across respondents using a random effects model or mean level data, in which explanatory variables were used to estimate the mean value given to each state. A set of binary dummy variables was created to describe each level and dimension of the health state. There was a binary dummy variable to take account of any additional effect on the health state value when one or more dimensions of health were at the most severe level. The models were estimated by the ordinary least square mean level model with constant forced through unity and by maximum likelihood for the random effects model, with the most severe term included to account for interactions. Explanatory power for the ordinary least square model was expressed in terms of an adjusted R-squared. The ability of the models to predict health state values was assessed in terms of mean absolute errors and the proportion of predictions outside 0.05 and 0.10 on either side of the actual value. Predictions were further tested in terms of bias using t-tests. Since the levels of each dimension were ranked progressively worse, the dummies represented progressively worse problems compared to a baseline with no problem for that dimension. Therefore, the coefficient estimates for the dummies on each dimension should be negative and increasing in size. An inconsistent result was one where a coefficient decreased rather than increased in size. All analyses were carried out in STATA 8.2.

Results

Over 14 months, 16 400 telephone calls were made, from which 6746 potential households were identified. Of these, the targeted individual was working overseas, had hearing or language problems precluding a telephone interview, could not be contacted after 10 attempts or another household member refused on their behalf, leaving 2544 targeted respondents who were contacted. Of these, 392 either

refused or gave incomplete responses and 2152 completed the initial telephone survey, giving a response rate for the telephone survey of 85% (2152/2544) of contacted target respondents or 32% (2152/6746) of possible cases.

Of the 2152 respondents who completed the telephone interview, 964 (45%) agreed to participate in the face-to-face interviews, of which 641 (66%) were eligible, willing and able to complete the interviews. Sex, age, living district, and smoking habit were similar between participants and non-participants, but the latter had lower educational qualifications (Table 1).

More severe role limitation was reported by participants and poorer social functioning by non-participants. Of the 641 participants in the face-to-face interviews, 29 (4.5%) were excluded because they failed to value the pits state and were therefore unable to generate an adjusted standard gamble value. A further 30 participants who gave the same valuation for each of the seven intermediate health states were also excluded, leaving 582 participants' data for analysis; each made eight standard gamble valuations giving 4656 valuations, of which 60 (1.3%) were illogical so 4596 valuations were finally analysed.

Table 1. Characteristics of participants and non-participants in the face-to-face interview

Variable	No. (%) of non-participants (n=1496)	No. (%) of participants (n=575)	P value, Chi-square test
Male	639 (43)	227 (40)	0.178
Age (years)			0.112
18-39	732 (49)	291 (51)	
40-64	486 (33)	201 (35)	
≥65	269 (18)	82 (14)	
Education level			<0.001
Tertiary	372 (25)	203 (36)	
Secondary	711 (48)	270 (47)	
Primary	276 (19)	84 (15)	
None	122 (8)	15 (3)	
Living district			0.078
Hong Kong	202 (14)	102 (18)	
Kowloon	481 (33)	176 (31)	
New Territories	775 (53)	296 (52)	
Smoking habit			0.177
Never	611 (78)	251 (83)	
Current	123 (16)	36 (12)	
Ex-smoker	49 (6)	15 (5)	

Table . Sample representativeness

Variable	% of sample (n=582)	% of population	Effect size*
Sex			0.19
Male	37.8	47.3	
Age (years)			0.18
18/15-24†	21.1	15.3	
25-34	15.8	17.7	
35-44	22.3	22.3	
45-54	16.2	19.9	
55-64	11.7	10.7	
≥65	12.9	14.1	
Highest education level			0.46
Primary	13.7	25.9	
Secondary	48.3	51.7	
Tertiary (non-degree)	17.4	07.6	
Tertiary (degree)	20.6	14.8	

* Effect size of 0.1=small, 0.3=medium, and 0.5=large
† Data for population are ≥15 years and for sample are ≥18 years

Comparisons were made between the final sample of respondents and the 2005 population[13] on sex, age and education (Table 2). The effect sizes for the variables of sex and age were 0.19 and 0.18, respectively, which were small and the sample was reasonably representative in these variables. However, the sample included more highly educated respondents than the general population, with a medium-to-large effect size of 0.46. Thus, the impact of weighting the sample by education level was examined.

Health state values

There were 158/197 (80%) health states with a median value greater than the mean, indicating that the data were skewed left.

Individual model

All beta coefficients had the expected negative sign in the model and were significant at the 10% level. There were three inconsistent coefficients: pain 2 to 3, pain 2 to 4, and mental health 2 to 3. In each case the higher level should have had a larger negative coefficient but did not. The UK model had four such inconsistencies. There was also evidence of some bias ($t \neq 0$) in the predictions of the random effects model, as there was in the UK study. However, the overall predictive ability was good with a mean absolute error of 0.070 compared to 0.078 in the UK study.

Mean model

All coefficients were significant and there were four inconsistencies: physical functioning 2 and 3, social functioning 2 and 3, pain 2 and 3, and mental health 4 and 5. For two of these, the difference was very small (0.001) and none were greater than 0.02. The predictive ability of the mean model was better than the individual model with a mean absolute error of 0.057 (compared to 0.075 in the UK study). As the mean was an ordinary least squares model, it was unbiased.

The performance of the Hong Kong models compared favourably with the UK models in terms of the mean absolute error and the number of absolute errors greater than 0.05 or 0.10. The results supported the validity of preference-based valuation of the SF-6D HK in the local population.

Improving the Hong Kong model

In order to generalise our model, weights were created by dividing the population proportion by the sample proportions by age, sex, and education. These weights were incorporated into the model in STATA. The coefficients from the weighted and unweighted models were similar, as were the mean absolute error and the number of absolute errors greater than 0.05 or 0.10.

Table 3. Coefficients for the consistent version of the mean model

SF-6D item*	Coefficients for the mean consistent model†
PF2	-0.050
PF3	-0.056
PF4	-0.092
PF5	-0.103
PF6	-0.178
RL2	-0.035
RL3	-0.035
RL4	-0.054
SF2	-0.039
SF3	-0.050
SF4	-0.050
SF5	-0.073
PAIN2	-0.037
PAIN3	-0.037
PAIN4	-0.052
PAIN5	-0.060
PAIN6	-0.100
MH2	-0.038
MH3	-0.058
MH4	-0.088
MH5	-0.088
VIT2	-0.039
VIT3	-0.056
VIT4	-0.063
VIT5	-0.077
Most severe level	-0.115

* PF denotes physical functioning, RL role limitations, SF social functioning, MH mental health, and VIT vitality

† All are significant at $t_{0.10}$

Final model for Hong Kong data

For the purpose of generating a model for use in cost utility analyses, the intercept to unity was restricted. The mean models appeared to be better than the individual models. The mean level model with the interaction term was therefore recommended. To deal with the few inconsistent values, the model was re-run to produce the consistent model (Table 3). To estimate the utility of a health state, these results were combined with a set of SF-36 data, and the specific health state can be described in terms of scores on the dimensions (Table 3). For example, if physical functioning scores level 2 (ie PF2) but all other dimensions score 1 (ie the best score), the utility is estimated by subtracting the coefficient 0.05 from 1, giving 0.95. If other dimensions score other than 1, then the relevant coefficients are combined to estimate the utility value of the health state.

Discussion

This study aimed to derive utility weights using a local population sample in such a way that they can be used to predict the value of any health state described by the locally validated SF-36. A standard gamble method was used to obtain the utility values in interviews with a final sample of 582 people. The sample underrepresented persons with lower levels of education but weighting made no appreciable difference to the results. Each individual valued a range of states of different predicted values so that further biases are unlikely.

In the standard gamble exercise, individuals were allowed time to understand and feel comfortable with the tasks. The proportion of participants who considered the quality of their answer poor or very poor was <2%, as was the proportion rated by the interviewer as not having understood the task. In the final model, some levels were re-grouped to produce a consistent algorithm for use. These inconsistencies should be further investigated to determine whether there are any implications for the wording of the SF-36 HK.

The mean model was considered as having better predictive ability, as the mean absolute error and number of absolute errors >0.05 or >0.10 were fewer when compared to the model with individual level data. The interaction terms were significant in both models and improved the predictive ability. In the comparison between the Hong Kong and UK models, there appeared to be some systematic difference in valuation in the two populations, for which more research is needed. A few interactions were also identified, but further investigation was limited because the number of observations required to do this exceeded the data available.

The results of this study provide a way of estimating a preference-based single index of utility for the health state of a Hong Kong sample. It gives an alternative to single index measures like the Health Utilities Index for those who would prefer to use the SF-36. It can also be applied retrospectively to existing SF-36 datasets.

Conclusions

Using the derived coefficients for the SF-6D health states, we can transform any set of SF-36 HK data to utility weights for the determination of QALYs. These QALYs are locally relevant and have a reasonable degree of validity. This enables calculations of costs per QALY for procedures and cost-utility analyses in any studies by using the SF-36 HK measures.

Acknowledgements

This study was supported by the Health and Health Services Research Fund (#02030351), Food and Health Bureau, Hong Kong SAR Government. We thank Prof A O'Hagan and Dr Samer A Kharroubi of the Centre for Bayesian Statistics in Health Economics, Department of Probability and Statistics, University of Sheffield for assistance in the selection of the health states to be included in the valuation exercise. We also thank those who have participated in the study.

References

1. Drummond MF, Stoddart GL, Torrance GW. Methods for the economic evaluation of health care programmes. Oxford: Oxford University Press; 1987.
2. Brook RH, Ware JE Jr, Rogers WH, et al. Does free care improve

adults' health? Results from a randomized controlled trial. N Engl J Med 1983;309:1426-34.
3. Tarlov AR, Ware JE Jr, Greenfield S, Nelson EC, Perrin E, Zubkoff M. The Medical Outcomes Study. An application of methods for monitoring the results of medical care. JAMA 1989;262:925-30.
4. Lam CL. Reliablity and construct validity of the Chinese (Hong Kong) SF-36 for patients in primary care. Hong Kong Pract 2003;25:468-75.
5. Lam CL, Chan MS, Ren XS, Gandek B. Chinese (Hong Kong) translation of the MOS 36-item short form health survey (SF36) standard version 1. October 1996. Revised May 1998.
6. Lam CL, Lauder IJ, Lam DTP, Gandek B. Validation and norming of the MOS 36-item Short Form Health Survey in Hong Kong Chinese adults. Health Services Research Committee Dissemination Report No. 711026. Hong Kong: Health Services Research Committee; November 2000.
7. Lam CL, Fong DY, Lauder IJ, Lam TP. The effect of health-related quality of life (HRQOL) on health service utilisation of a Chinese population. Soc Sci Med 2002;55:1635-46.
8. Lam CL, Tse EY, Gandek B. Is the standard SF-12 Health survey valid and equivalent for a Chinese population? Qual Life Res 2005;14:539-47.
9. Lam CL, Tse EY, Gandek B, Fong DY. The SF-36 summary scales were valid, reliable, and equivalent in a Chinese population. J Clin Epidemiol 2005;58:815-22.
10. Brazier J, Usherwood T, Harper R, Thomas K. Deriving a preference-based single index from the UK SF-36 Health Survey. J Clin Epidemiol 1998;51:1115-28.
11. Lam CL, Brazier J, McGhee SM. Valuation of the SF-6D health states is feasible, acceptable, reliable, and valid in a Chinese population. Value Health 2008;11:295-303.
12. Brazier J, Roberts J, Deverill M. The estimation of a preference-based measure of health from the SF-36. J Health Econ 2002;21:271-92.
13. Hong Kong Census and Statistics Department. Women and men in Hong Kong: key statistics, 2006.

NLS Tang 鄧亮生
CY Chan 陳超揚
CC Leung 梁子超
CM Tam 譚卓明
J Blackwell

Tuberculosis susceptibility genes in the chemokine cluster region of chromosome 17 in Hong Kong Chinese

Key Messages

1. There was a borderline association between a single nucleotide polymorphism (SNP) located within the CCL1 gene and predisposition to tuberculosis using a single-point analysis. The association was no longer significant when the effect of multiple statistical testing was taken into account.
2. This SNP was also associated with tuberculosis diagnosed in young patients (<35 years old).
3. This SNP was not associated with other clinical features such as smear positivity and extent of disease.

Hong Kong Med J 2011;17(Suppl 6):S22-5

Faculty of Medicine, The Chinese University of Hong Kong:
Department of Chemical Pathology
NLS Tang
Department of Microbiology
CY Chan
Tuberculosis and Chest Service, Department of Health, Hong Kong
CC Leung
Genetics and Infection Laboratory, Cambridge Institute of Medical Research, University of Cambridge, United Kingdom
J Blackwell

RFCID project number: 03040512

Principal applicant and corresponding author:
Prof Nelson LS Tang
Department of Chemical Pathology, Faculty of Medicine, The Chinese University of Hong Kong, Shatin, NT, Hong Kong SAR, China
Tel: (852) 2632 2960
Fax: (852) 2636 5090
Email: nelsontang@cuhk.edu.hk

Introduction

Tuberculosis (TB) is a major global health concern, particularly in the Asia Pacific region. Host genetic factors play an important role in the predisposition and prognosis for infectious diseases, in addition to factors such as the environment, pathogen virulence, and public health status.

Genetic variation of disease predisposition is largely determined by single-base variants in our genome, known as single nucleotide polymorphisms (SNPs). One third of the population has been exposed to *Mycobacterium tuberculosis*, but only 10% of them go on to develop the disease.[1,2] Monozygotic twins were more likely to develop TB or not at all together (concordance) than dizygotic twins, indicating an underlying genetic trait of susceptibility to TB.[3]

Several genes contributing to the susceptibility to TB have been identified, including *SLC11A* (also known as *NRAMP1*). This gene was first identified for its role in susceptibility to multiple intracellular pathogens in mice, and later mapped to chromosome 2q35 in humans. Its function has been reviewed.[4] Other than *SLC11A1*, genes involved in immune reaction and familial predisposition to TB are also potential susceptibility genes in sporadic TB. They include the signalling pathway of interferon gamma (IFNγ) and other cytokines.[5] Other predisposing genes found in sporadic cases entail the vitamin D receptor, IL12B, and other cytokines/chemokines.[4]

Familial studies suggest that one or more chemokine genes in the chemokine cluster regions in chromosome 17q11.2 might be associated with susceptibility to TB or mycobacterial disease. However, the exact identity and location of the predisposing gene is not known. To delineate the causative predisposing gene(s), genetic association studies in other populations are needed. We therefore used a tagging SNP approach to study the association between CCL chemokine genes and susceptibility to TB, and between the clinical phenotype and disease severity.

Methods

This genetic association study was conducted from 1 November 2005 to 31 October 2007. Tagging genetic polymorphisms (tagSNPs) were defined and genotyped in the whole sample set of 1040 TB cases and >1000 controls.

Hong Kong Chinese attending the territory-wide Chest Clinic of the Tuberculosis and Chest Service with confirmed TB were invited to participate. Ethical approval was obtained from The Chinese University of Hong Kong and the Hong Kong Department of Health in 2002. Informed written consent was obtained from each subject. Blood samples were collected, and clinical parameters about the extent and severity of disease were recorded.

Inclusion criteria were smear and/or culture and/or clinical symptoms positive for TB, according to the diagnostic criteria of the International Union against Tuberculosis and Lung Diseases with clinical-radiological and histological evidence and clinical responses to treatment. Patients with HIV or other immunodeficiencies were excluded.

A tagging SNP approach was used to select informative SNPs for genotyping of the whole sample set. All SNP data were extracted from dbSNP and International HapMap Project both at the time when this project started in November 2005 and subsequently in January 2006 when the HapMap Project released the Phase II results. A spectral decomposition algorithm was used to identify the location of SNPs that are important to delineate the overall genetic variations in this region. A total of 30 factors (composition of SNPs) were identified at this stage covering the genomic regions, including coding and non-coding region of the genes. The SNPs entered into these 30 factors were genotyped by polymerase chain reaction (PCR)–restriction fragment length polymorphism (PCR-RFLP), allele-specific PCR (AS-PCR) or PCR-DNA sequencing.

Genomic DNA was extracted from peripheral blood using the DNA extraction kit according to the manufacturer's instruction. Genotyping was performed by PCR-RFLP, AS-PCR, TaqMan assay, or PCR-DNA sequencing. In brief, the PCR entailed 25 μL reactions comprising 0.25 mM of each primer pair, 2 mM $MgCl_2$, 1U of Ampli Taq Gold Polymerase (Applied Biosystems) and PCR buffer (10 mM Tris–HCl, pH 8.3; 50 mM KCl). The reaction cycle was started at 96ºC for 15 min to activate the polymerase, and amplification was achieved by 35 cycles at 96ºC for 30 s, annealing temperatures for 45 s and 72ºC for 45 s. The final elongation step was at 72ºC for 7 min. For restriction enzyme digestion, 7 μL of the PCR product was digested overnight by 5 to 10 U of the required enzyme. The genotype call was made by separating the DNA in a 4% agarose gel and stained with ethidium bromide.

For AS-PCR and melting analysis, there were two separate allele-specific primers in each reaction, together with a common reverse primer. Each of the two allele-specific primers hybridised to one specific allele of the SNP and produced a PCR product whenever such an allele was present in the DNA template. The products produced from the pair of allele-specific primers were differentiated from each other by a different melting temperature, as different numbers of GC bases were incorporated into the 5' end of the primer. The intercalating dye SYBR Green was used to monitor the melting profile of the PCR product and a melting curve profile was generated in a real-time thermocycler (ABI-7900HT) after completion of 35 cycles of standard PCR.

Some SNPs were also genotyped using TaqMan SNP Genotyping Assays (Applied Biosystems, USA). This assay used two probes with different fluorescent dyes that bind to two alleles of the SNP. One probe labelled with VIC dye detected the Allele 1 sequence, and the other labelled with the FAM dye detected the Allele 2 sequence. By using the 5´ nuclease assay, the products were amplified and the specific SNP alleles could be detected in purified genomic DNA samples.

Sequencing of PCR products was performed by BigDye Terminator Cycle sequencing kits with an ABI-3100 autosequencer (Applied Biosystems, USA). The sequencing reaction cycles were performed according to the manufacturer's instructions.

Statistical analysis of genotype distribution was performed by the Chi-square test for trend, assuming an additive model of allelic risk. The Hardy-Weinberg equilibrium test for genotype distribution was performed by the Chi-square test with 1 df. Univariate associations between categorical clinical features and genotypes were performed using the Chi-square test. Odds ratios (ORs) and 95% confident intervals (CIs) were also calculated. To correct for multiple testing, the Bonferroni correction was applied to provide a corrected P value at significant level of 0.05. Therefore, only those associations with empirical P values of <0.0016 (ie 0.05/30 tagSNPs or independent tests) were considered significant. Haplotype evaluation was performed with a haploview program.[4] Spectral decomposition was performed using statistical software R.

Results

The mean age of the patients was 48.3 (standard deviation, 19.4) years. The male gender was predominant (695 males vs 345 females). About 88% of the patients were new cases. The smear positive group consisted of 344 patients. Among patients with pulmonary TB, the extent of lung involvement was minimal (less than the right upper lobe) in 67%, moderate (more than the right upper lobe) in 25%, and severe (more than one lung) in 8%, based on chest radiography at the time of diagnosis.

Within the proximity of the 14 candidate chemokines genes, the pattern of LD was evaluated by the Haploview program. There was LD within the following clusters of genes present inside different haploblocks: CCL2-CCL7-CCL11, CCL8, CCL13-CCL1, CCL5, CCL16, CCL14, CCL15-CCL23, CCL18, CCL3-CCL4. After application of the spectral decomposition algorithm for tagSNP selection, 30 tagSNPs were identified to represent most of the genetic variations in the candidate regions.

Association between genetic polymorphisms and predisposition to tuberculosis

In the whole sample set, a total of 30 tagSNPs were selected for genotyping. This set of tagSNPs provided a comprehensive coverage of the genetic variation of the chemokine gene clusters in chromosome 17q11.2. A borderline association was detected between an SNP (rs2282691) located in intron of CCL1 gene and TB predisposition using a single-point chi-square for trend analysis (P=0.006, Fig). The frequency of the minor allele was lower in the control group (0.27) than in the patient group (0.31). Nonetheless, the association was not significant after correction of multiple testing by the Bonferroni method (corrected P=0.16). The minor allele

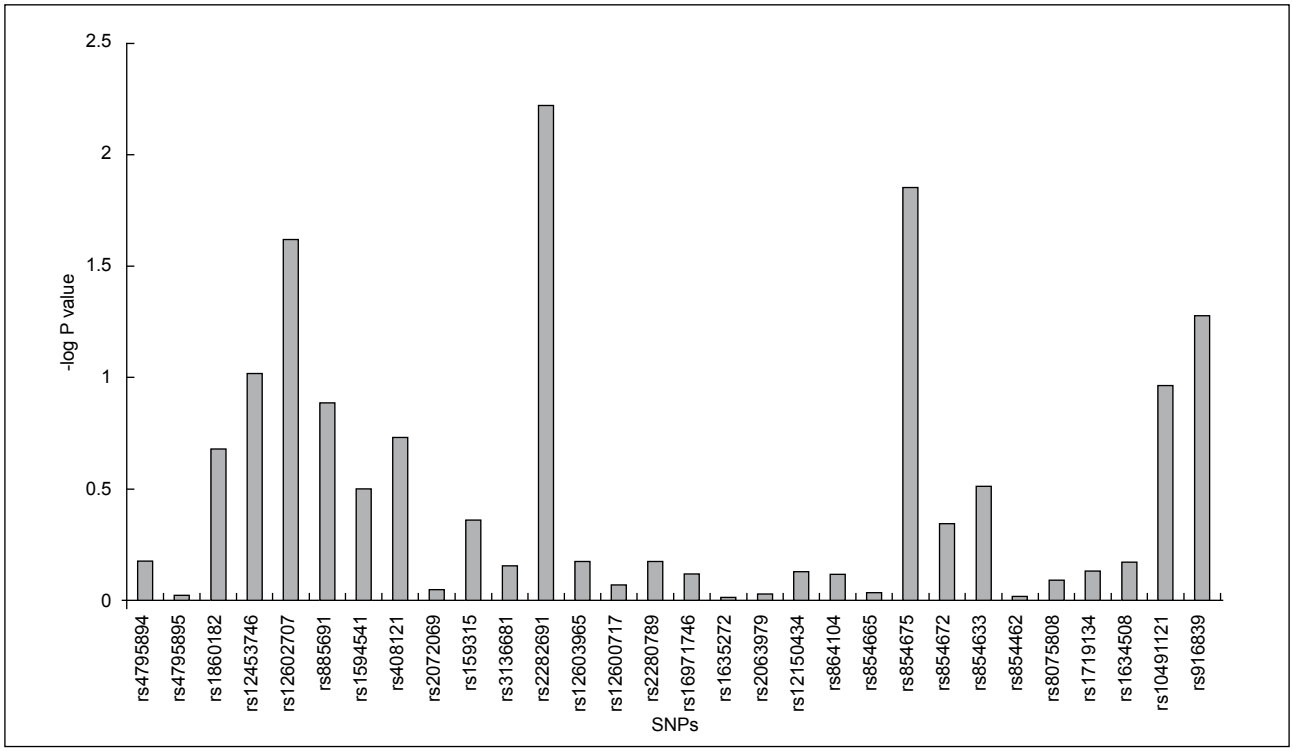

Fig. Strength of association among the tagSNPs
The P values are plotted as –log values, so a high peak represents a strong association. The most significant association was found on the tagSNP rs2282691

carried a 1.19-fold increase in risk of TB (95% CI, 1.05-1.36).

As young TB patients may have a strong genetic predisposition, patients within the lowest tertile of onset age (ie <35 years) were defined as early onset, and the association with genotypes was examined again as categorical groups. The CCL1 was also associated with disease predisposition in early-onset patients (P trend=0.00013, Table 1). Genotypes followed the Hardy-Weinberg equilibrium in both groups.

Association between clinical parameters and genotypes

The CCL1 predisposing SNPs were also examined for potential association with disease phenotype and severity. The predisposing SNP (rs2282691) was not associated with smear positivity (P=0.8) when comparing the 344 smear positive patients with the remaining patients.

The extent of pulmonary TB was categorised into three grades to examine the association between genotypes and the extent of disease, using the Chi-square test for trend. The SNP was not associated with the extent of disease on radiographs (P for trend=0.1).

Among patients with and without pulmonary cavity, a moderate association was found (P trend=0.01, Table 2). This was consistent with the association with predisposition to TB infection that the "A" allele was also the high-risk allele for development of a cavity.

Table 1. Association between tuberculosis in young patients and single nucleotide polymorphism (rs2 82691) in CCL1

Case vs control	rs2282691		
	AA	AT	TT
No. (%) of controls	65 (6.3)	368 (35.9)	593 (57.8)
No. (%) of young tuberculosis patients (age <35 years)	30 (9.5)	142 (44.9)	144 (45.6)

Table . Association between pulmonary cavity and single nucleotide polymorphism (rs2 82691) in CCL1

Case vs control	rs2282691		
	AA	AT	TT
No. (%) of patients without pulmonary cavity	67 (9.5)	292 (41.2)	349 (49.3)
No. (%) of patients with pulmonary cavity	21 (14.6)	66 (45.8)	57 (39.6)

Discussion

The genetic association of the tagging SNP located inside intron 2 of CCL1 with TB was of borderline significance. This SNP was associated with predisposition in young-onset patients and with disease severity. It was also located in proximity to CCL13, in addition to CCL1. This suggested that both genes might be important mediators in the host defense against TB. Young-onset patients appeared to represent a more homogeneous group of patients under stronger genetic influence.

Both innate and adaptive immunity are activated in TB infection. Activation of the Toll-like receptor (TLR) system is the first key innate response.[6] The TLR2, together with other TLRs, interacts with lipoprotein and other secreted antigens of TB and leads to induction of a battery of cytokines, including IL-6, IL-10, TNFα, and IL-12. These are followed by activation of acquired immunity, which includes $CD4^+$ T cell involvement. In addition to signalling through the TLRs, additional receptors and signals also play important roles. Type 1 interferon receptors and STAT1 are also activated in macrophages leading to activation of a battery of chemokines, including RANTES, IP-10, and MIG.[7] Subsequent induction of interferon γ in Th1 cells potentiates macrophage phagosomal lytic activity in an attempt to kill TB by expression of NOS2. Many interferon inducible genes and chemokines are activated as a result of this variety of host responses to TB. These findings support an essential role of chemokines in host defence against TB.

In animal models, mycobacteria-infected macrophages are induced to produce a whole panel of chemokines (CCL1 to CCL5, CCL7, CCL8, CCL13).[8] These chemokines are also found in bronchial lavage of TB patients, confirming their functional importance in the immune reaction to TB in humans.[9,10]

Chemokines are involved in the differentiation into Th1 and Th2 immune response. Different chemokines are activated when exposed to different antigens (mycobacteria and Schistosoma) and subsequently lead to formation Th1 or Th2 granulomas in mice.[11] Induction of CCL1 is associated with the formation of Th2 granulomas. CCL1 is expressed and secreted by monocytes and binds to CCR8, which is highly expressed among polarised Th2 cells and regulatory T cells.[12] Thus activation of CCR8 by CCL1 leads to a Th2 immune response. However, host defence against TB and autophagy requires induction by Th1, which is inhibited by Th2 cytokines.[13] Therefore, we postulate that individuals with preferential activation/expression of CCL1 are likely to over-express a Th2 phenotype in response to pathogens (including TB) and inappropriately inhibit the required Th1 response. Future functional studies are required to confirm this hypothesis.

It is important to confirm this borderline significant association in another sample set, with much larger samples of cases and controls. Other sample sets with no bias on clinical diagnostic features may be useful to confirm the association with clinical disease severity. Functional genetic study is needed to elaborate on the mechanism underlying the predisposition or protective effect of this genetic variation.

Acknowledgements

This study was supported by the Research Fund for the Control of Infectious Diseases (#03040512), Food and Health Bureau, Hong Kong SAR Government. We thank all patients and health care workers who participated in this study.

References

1. Murray CJ, Styblo K, Rouillon A. Tuberculosis in developing countries: burden, intervention and cost. Bull Int Union Tuberc Lung Dis 1990;65:6-24.
2. Bloom BR, Murray CJ. Tuberculosis: commentary on a reemergent killer. Science 1992;257:1055-64.
3. Jepson A, Fowler A, Banya W, et al. Genetic regulation of acquired immune responses to antigens of *Mycobacterium tuberculosis*: a study of twins in West Africa. Infect Immun 2001;69:3989-94.
4. Bellamy R. Susceptibility to mycobacterial infections: the importance of host genetics. Genes Immun 2003;4:4-11.
5. Blackwell JM, Searle S, Mohamed H, White JK. Divalent cation transport and susceptibility to infectious and autoimmune disease: continuation of the Ity/Lsh/Bcg/Nramp1/Slc11a1 gene story. Immunol Lett 2003;85:197-203.
6. Barrett JC, Fry B, Maller J, Daly MJ. Haploview: analysis and visualization of LD and haplotype maps. Bioinformatics 2005;21:263-5.
7. Sen J. Taking Toll of TB. Trends Immunol 2001;22:297-8.
8. Shi S, Blumenthal A, Hickey CM, Gandotra S, Levy D, Ehrt S. Expression of many immunologically important genes in *Mycobacterium tuberculosis*-infected macrophages is independent of both TLR2 and TLR4 but dependent on IFN-alphabeta receptor and STAT1. J Immunol 2005;175:3318-28.
9. Chiu BC, Freeman CM, Stolberg VR, et al. Cytokine-chemokine networks in experimental mycobacterial and schistosomal pulmonary granuloma formation. Am J Respir Cell Mol Biol 2003;29:106-16.
10. Sadek MI, Sada E, Toossi Z, Schwander SK, Rich EA. Chemokines induced by infection of mononuclear phagocytes with mycobacteria and present in lung alveoli during active pulmonary tuberculosis. Am J Respir Cell Mol Biol 1998;19:513-21.
11. Kurashima K, Mukaida N, Fujimura M, et al. Elevated chemokine levels in bronchoalveolar lavage fluid of tuberculosis patients. Am J Respir Crit Care Med 1997;155:1474-7.
12. Sironi M, Martinez FO, D'Ambrosio D, et al. Differential regulation of chemokine production by Fcgamma receptor engagement in human monocytes: association of CCL1 with a distinct form of M2 monocyte activation (M2b, Type 2). J Leukoc Biol 2006;80:342-9.
13. Harris J, De Haro SA, Master SS, et al. T helper 2 cytokines inhibit autophagic control of intracellular *Mycobacterium tuberculosis*. Immunity 2007;27:505-17.

PKS Chan 陳基湘
S Ma 文子光
SM Ngai 倪世明

Identification of T-cell epitopes of SARS-coronavirus for development of peptide-based vaccines and cellular immunity assessment methodse

Key Messages

1. Subjects recovered from SARS-CoV infection retain memory of cellular immune response to epitopes spanning over a few regions of the viral nucleoprotein. Ten such epitopes were identified.
2. The majority of epitopes were predominantly recognised by $CD8^+$ cytotoxic T cells and elicited persistent memory response lasting at least 2 years.
3. There is potential to use the nucleoprotein of SARS-CoV to develop vaccines and diagnostic assays based on such cellular immune responses.

Introduction

Severe acute respiratory syndrome (SARS) killed more than 800 people during a global outbreak in 2003. Specific antiviral treatment and prophylactic vaccine for SARS coronavirus (CoV) are not available. Among proteins encoded by the CoV family, the nucleoprotein is the most abundantly expressed and immunodominant. The nucleoprotein of SARS-CoV is crucial in the infection and pathogenic process, and is a highly sensitive diagnostic tool to detect SARS-CoV-specific antibody production.

Although the SARS-CoV nucleoprotein does not induce neutralising antibody, a nucleoprotein-specific cytotoxic T lymphocyte response is present in individuals who recovered from the disease. There is a potential to induce such an immune response by vaccination. This study examined the cytotoxic T lymphocyte epitopes of nucleoproteins from subjects who recovered from the SARS outbreak in Hong Kong in 2003.

Methods

This study was conducted from 1 October 2005 to 30 September 2007. We recruited 55 subjects who had recovered from SARS-CoV infection and 10 controls without a history of SARS and tested negative for SARS-CoV-specific antibodies. A peripheral blood sample was collected 3, 10 to 12, and 22 to 24 months after the onset of illness for peripheral blood mononuclear cell (PBMC) extraction.

The interferon-gamma (IFN-γ) release enzyme-linked immunospot (ELISpot) assay was used to measure T-cell response to in vitro stimulation with peptides derived from the SARS-CoV nucleoprotein. The MultiScreen IP plate (Milipore, Bio-Gene) was coated with human IFN-γ capture antibodies (R&D Systems). Cryo-preserved PBMCs were thawed and resuspended in culture medium RPMI 1640 containing 10% human AB serum (Sigma). A 100-μL aliquot containing $1.5x10^5$ viable cells was seeded per well (in triplicate) and mixed with testing peptides at a final concentration of 10 μg/mL. Concanavalin A (Sigma) at 0.5 μg per well was used as a mitogen control. The positive peptide pool comprised 12 peptides derived from cytomegalovirus and Epstein-Barr virus. Cell controls were PBMCs alone without pulsing with any peptide. After an overnight incubation, the plate was washed. Human IFN-γ detection antibody (R&D Systems) was added to each well and incubated overnight at 4ºC. On the next day, the plate was washed, followed by the addition of streptavidin-alkaline phosphate. After 2 hours of incubation at room temperature, the plate was washed again and followed by colour development using the Human INF-gamma ELISpot development module (R&D Systems). The net number of IFN-γ–producing cells for each peptide-test well was obtained by subtracting the mean spot-forming cell (SFC) counts of the corresponding triplicate cell control wells. A peptide or peptide pool was regarded as producing a positive response when the average net SFC count of the triplicate peptide test wells was greater than the mean plus two standard deviations (SD) of the cell controls, and having at least 20 SFCs.

Hong Kong Med J 2011;17(Suppl 6):S26-30

The Chinese University of Hong Kong:
Department of Microbiology
PKS Chan
Department of Biology
SM Ngai
Section of Infection and Immunity, University of Wales College of Medicine, Cardiff, United Kingdom
S Ma

RFCID project number: 03040602

Principal applicant and corresponding author:
Prof Paul KS Chan
Department of Microbiology, The Chinese University of Hong Kong, 1/F Clinical Science Building, Prince of Wales Hospital, Shatin, New Territories, Hong Kong SAR, China
Tel: (852) 2632 3333
Fax: (852) 2647 3227
Email: paulkschan@cuhk.edu.hk

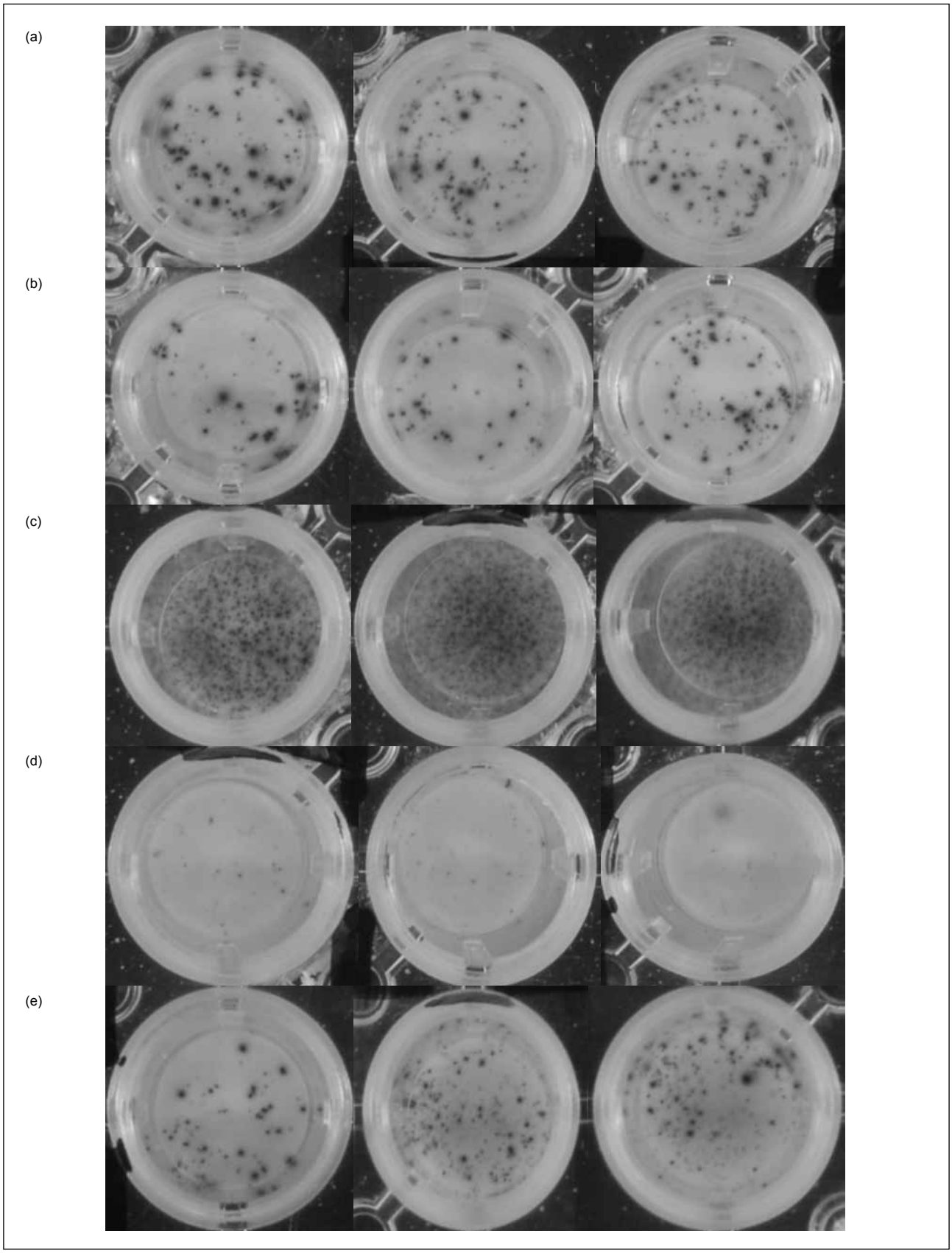

Fig 1. Typical examples of INF-γ–producing cells detected by ELISpot assay 3 months after onset of SARS
Each IFN-γ–producing cell appears as a dark spot with solid centre and faint border. (a) P-18 (containing peptide N48) and (b) P-21 (containing peptide N63) peptide pools show positive screening results and responses on fine mapping. (c) Peripheral blood mononuclear cells (PBMCs) stimulated with Concanavalin A, which is a mitogen to serve as a positive control to indicate cells, are viable and capable of producing INF-γ. (d) Cell controls are PBMCs not pulsed with any peptide. (e) Positive peptide pool (containing cytomegalovirus and Epstein-Barr virus T-cell epitopes) is recognised by HLA types commonly found in southern Chinese

Table. Response to SARS-CoV nucleoprotein-derived peptides measured by IFN-γ ELISpot assay in subjects who recovered from SARS

Peptide name	% of subjects with a positive response in spot-forming cell counts			
	HLA-A*02 phenotype (n=28)	HLA-A*11 phenotype (n=25)	HLA-A*24 phenotype (n=13)	HLA-A*33 phenotype (n=8)
N15 (amino acid position 71-85)	0	8.0	15.4	0
N17 (amino acid position 81-95)	0	8.0	0	0
N18 (amino acid position 86-100)	10.7	24.0	92.3	0
N22 (amino acid position 106-120)	0	4.0	7.7	0
N25 (amino acid position 121-135)	3.6	0	0	0
N48 (amino acid position 236-250)	21.4	72.0	23.1	0
N53 (amino acid position 261-175)	3.6	12.0	0	37.5
N63 (amino acid position 311-325)	85.7	48.0	30.8	25.0
N68 (amino acid position 336-350)	28.6	20.0	0	75.0
N71 (amino acid position 351-365)	25.0	24.0	0	87.5

Peptides used were 15-mer overlap by 10 amino acids covering the whole nucleoprotein, except the last two amino acids at the C-terminus. The 3-month samples were screened with peptide pools. Subjects showing positive results were further tested with individual peptides. To determine the longevity of immune response memory, the 1-year and 2-year samples were tested in parallel against the reactive peptides. To further characterise the identified T-cell epitopes, PBMCs were pretreated to select $CD8^+$ cells and retested in parallel with the whole PBMC preparation.

Results

Of the 55 subjects, 26 males and 26 females aged 21 to 48 (mean, 29; SD, 7.2) years had provided complete follow-up samples. The phenotype frequencies were as follows: A*11 (61.5%), A*02 (53.8%), A*24 (17.3%), A*33 (15.4%); A*01, A*03, and A*30 (3.8% each); and A*26, A*29, A*31 (1.9% each). The phenotype frequencies for DRB1 were as follows: DRB1-09 (40.4%), -12 (32.7%), -15 (21.2%), -04 (23.1%), -14 (17.3%), -11 (11.5%), -08 and -16 (7.7% each), -03 and -07 (5.8% each), and -10 (3.8%).

Peptide pool screening

All subjects who recovered from SARS showed positive screening results to at least one peptide pool. The SFC counts for the peptide pools were 12 to 198 per $1.5x10^5$ PBMCs, whereas those for the cell controls were 0 to 12 per $1.5x10^5$ PBMCs. A typical example of ELISpot results is shown in Fig 1.

Fine epitope mapping

The 3-month samples were further tested with individual peptides selected according to the screening results. Ten peptides were found to produce a positive ELISpot. The overall positive rates were: N63 (24 of 52 subjects, 46.2%), N48 (34.6%), N68 (25.0%), N18 (23.1%), N71 (21.2%), N53 (7.7%), N15 and N17 (3.8% each), N22 and N25 (1.9% each). The positive rates according to HLA phenotyping are shown in the Table. None of the controls showed positive ELISpots.

Cross-sectional and longitudinal analyses on peptide response

The five peptides (N18, N48, N63, N68, and N71) that showed most frequent positive response were tested with the 1-year and 2-year PBMC samples to define the longevity of the T-cell response memory. Overall, the median SFC counts were 40 to 70 (range, 20-168) per $1.5x10^5$ PBMCs. To compare the response between peptides, the SFC counts for the five peptides obtained from PBMCs collected at 3 months post-illness onset were not significantly different (P=0.293, Kruskal-Wallis test). Similarly, the SFC counts for 1-year and 2-year time points were not significantly different (P=0.187 for 1-year, P=0.434 for 2-year, Fig 2). Similarly, the SFC counts for each peptide across the three specimen collection time points were not significantly different (Kruskal-Wallis test).

$CD8^+$ cell enrichment

Five subjects showed a strong response to the corresponding peptide and had sufficient cells remaining for the $CD8^+$ cell enrichment study to characterise the five major epitopes identified. There was an increase in median SFC count for the $CD8^+$ cell-enriched preparation from 82 to 195 per $1.5x10^5$ cells for N18, from 76 to 210 for N48, from 102 to 315 for N63, from 66 to 155 for N68, and from 62 to 205 for N71.

Discussion

Infection with SARS-CoV induced T-cell response memory targeting the nucleoprotein. There were 10 T-cell epitopes located within four regions (residues 71-100, 106-135, 236-175, and 336-365) of the nucleoprotein. These epitopes were mainly HLA type-specific where A*02 recognised an epitope within residues 311-325 (N63), A*11 within residues 236-250 (N48), A*24 within residues 86-100 (N18), and A*33 within residues 351-365 (N71).

A similar approach identified T-cell epitopes within residues 331-347, 339-354, and 346-362.[1] The residues 331-347 and 339-354 corresponded to the N68 peptide, in

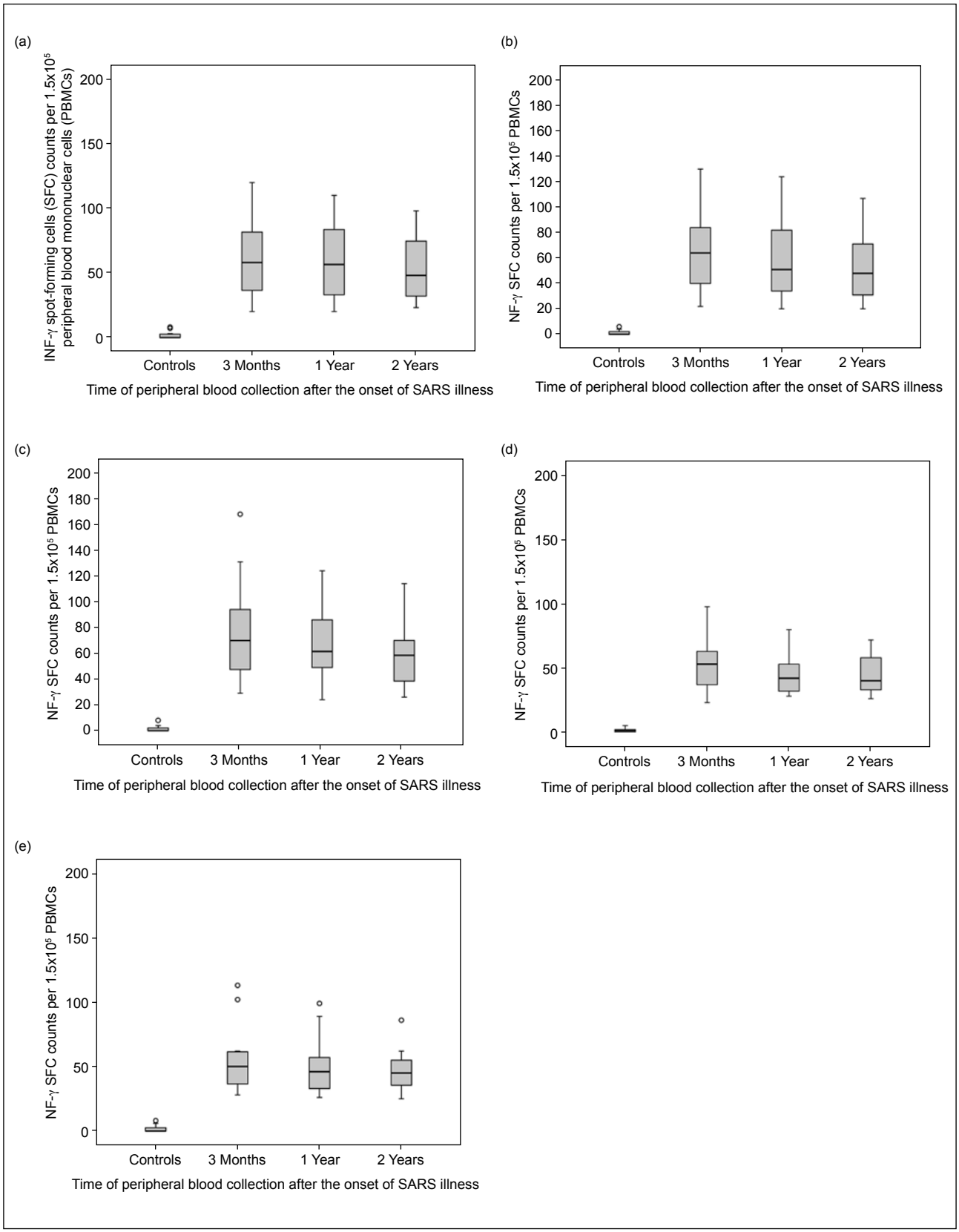

Fig 2. Frequency of INF-γ–producing cells in response to SARS-CoV nucleocapsid peptide stimulation according to the time of blood-sample collection*

(a) N18 (amino acid position 86-100) for 12 subjects who recovered from SARS and 10 controls, (b) N48 (amino acid position 236-250) for 18 subjects who recovered from SARS and 10 controls, (c) N63 (amino acid position 311-325) for 24 subjects who recovered from SARS and 10 controls, (d) N68 (amino acid position 336-350) for 13 subjects who recovered from SARS and 10 controls, and (e) N71 (amino acid position 351-365) for 11 subjects who recovered from SARS and 10 controls

* Circles represent outliers. None of the 10 non-SARS controls shows a positive response

line with the earlier study.[1] N68 elicited responses in A*02, A*11 and A*33 subjects. The peptide N63 (residues 311-325) predominantly recognised by A*02 subjects is able to induce recall memory from $CD8^+$ T cells.[2] The A*33-associated peptide N71 (residues 351-265) is immunogenic in a mouse model.[3] Several helper T-cell epitopes based on a mouse model have been identified,[3] including one located within residues 111-125, which overlaps with our peptide N22 that was shown to elicit a positive response in 4.0% of A*11 and 7.7% of A*24 subjects.

An A*02 epitope was predicted at residues 227-235 based on a T2 cell-peptide binding assay, but no significant response was observed when this peptide was tested with the PBMCs collected from four A*02 subjects using the IFN-γ release ELISpot assay.[4] We also did not observe a positive result towards this peptide—N46—from our tested subjects (including the 28 individuals with the A*02 phenotype). Given the concurrent results from this and previous studies,[4] residues 227-235 are unlikely to represent a T-cell epitope.

Another A*02 epitope was identified within residues 220-228 based on bioinformatics, and showed that a DNA vaccine encoding this epitope could induce cytotoxic immunity in a mouse model.[5] This potential peptide is within the N44 in our peptide pool, but no positive response was observed. Whether the spectrum of immune response between natural infection and vaccination differs remains to be defined. Our ELISpot results did not reveal a significant difference in SFC counts among samples taken 3 months, 1 year, and 2 years after the onset of illness. An immune response memory was detected from PBMC samples taken 2 years after the onset of illness.[1] Thus, cellular immune response memory following SARS-CoV infection persists for a substantial period (at least 2 years). Although the humoral immune response memory was not measured, it is likely that it too persists. These are encouraging observations for the development of a vaccine for SARS-CoV infection.

Acknowledgement

This study was supported by the Research Fund for the Control of Infectious Diseases (#03040602), Food and Health Bureau, Hong Kong SAR Government.

References

1. Peng H, Yang LT, Wang LY, et al. Long-lived memory T lymphocyte responses against SARS coronavirus nucleocapsid protein in SARS-recovered patients. Virology 2006;351:466-75.
2. Tsao YP, Lin JY, Jan JT, et al. HLA-A*0201 T-cell epitopes in severe acute respiratory syndrome (SARS) coronavirus nucleocapsid and spike proteins. Biochem Biophys Res Commun 2006;344:63-71.
3. Zhao J, Huang Q, Wang W, Zhang Y, Lv P, Gao XM. Identification and characterisation of dominant helper T-cell epitopes in the nucleocapsid protein of severe acute respiratory syndrome coronavirus. J Virol 2007;81:6079-88.
4. Zhou M, Xu D, Li X, et al. Screening and identification of severe acute respiratory syndrome-associated coronavirus-specific CTL epitopes. J Immunol 2006;177:2138-45.
5. Cheung YK, Cheng SC, Sin FW, Chan KT, Xie Y. Induction of T-cell response by a DNA vaccine encoding a novel HLA-A*0201 severe acute respiratory syndrome coronavirus epitope. Vaccine 2007;25:6070-7.

MCW Chan 陳志偉
RWY Chan 陳韻怡
GSW Tsao 曹世華
JSM Peiris 裴偉士

Pathogenesis of SARS coronavirus infection using human lung pithelial cells: an in vitro modele

Key Messages

1. In vitro models of well-differentiated bronchial epithelial cells and alveolar type II and type I–like pneumocytes were set up.
2. The SARS-CoV could replicate in well-differentiated bronchial epithelial cells and alveolar type II pneumocytes only.
3. In well-differentiated bronchial epithelial cells, type I interferons (interferon-beta) and cytokine and chemokines (eg RANTES, IP-10, IL-6, IL-8, MCP-1, MIP-1α, MIP-2α) were markedly induced after infection with SARS-CoV, compared to human coronavirus HCoV229E and influenza A (H1N1) virus.

Introduction

Severe acute respiratory syndrome (SARS) affected more than 8000 patients in over 32 countries. One third of the patients spontaneously recovered early in the course of disease; others progressed and about 30% needed intensive care. The aetiological agent was the SARS-coronavirus (SARS-CoV).[1,2] Experimental infection of cynomologous macaques with SARS-CoV reproduced a disease with diffuse alveolar damage and multi-nucleate syncytia reminiscent of human SARS.[3] The SARS-CoV has been demonstrated by reverse transcriptase polymerase chain reaction (RT-PCR) and virus isolation in respiratory secretions, faeces, urine, and lung biopsy, indicating that SARS-CoV is a disseminated infection rather than being restricted to the respiratory tract.

The virus antigen can be demonstrated in pneumocytes of SARS patients dying within the first 10 days of illness.[4] The predominant cells infiltrating the alveoli are CD68-positive cells. This suggests that alveolar pneumocytes may be the target cells of SARS-CoV and play a role in the pathogenesis of the disease. The SARS-CoV cannot replicate in differentiated respiratory epithelial cells or in primary non-differentiated bronchial and alveolar epithelial cells, even when its functional receptor—ACE2—is present (unpublished data).[5] It is therefore important to study virus-cell interactions in primary lung alveolar epithelial cells.

We have established differentiated models of human bronchial epithelial cells and have isolated the differentiated status of human types I and II pneumocytes. An ex vivo model for lung culture was also established to address the tropism and pathogenesis of SARS-CoV in human respiratory epithelial cells.

We aimed to establish (1) an in vitro model for primary human alveolar types I and II epithelial cells (pneumocytes), (2) an in vitro model for well-differentiated bronchial epithelial cells, and (3) an ex vivo model for SARS-CoV–infected human lung tissue culture. In addition, we aimed to define the gene expression profile (cytokine, chemokine) of primary human respiratory epithelial cells infected with SARS-CoV and compare it with human coronavirus 229E and influenza H1N1 virus.

Methods

This study was conducted from January 2006 to December 2007. Primary human respiratory epithelial cells were infected with SARS-CoV in vitro. Virus replication was monitored by measuring the levels of the SARS nucleocapsid genes, by immunofluorescence detection of the SARS-CoV nucleoprotein, and by titration of the infectious virus. The gene and protein expression profiles (cytokine and chemokine) of respiratory epithelial cells infected with SARS-CoV, human coronavirus 229E, and influenza A (H1N1) virus were compared using real-time quantitative RT-PCR.

Results

To evaluate SARS-CoV infection in human respiratory tract, ex vivo models for human lung culture and in vitro models for well-differentiated and polarised

Hong Kong Med J 2011;17(Suppl 6):S31-5

LKS Faculty of Medicine, The University of Hong Kong:
Department of Microbiology
MCW Chan, RWY Chan, JSM Peiris
Department of Anatomy
GSW Tsao

RFCID project number: 03040712

Principal applicant and corresponding author:
Dr Michael CW Chan
Department of Microbiology, LKS Faculty of Medicine, The University of Hong Kong, Pokfulam, Hong Kong SAR, China
Tel: (852) 2819 9800
Fax: (852) 2855 1241
Email: mchan@hkucc.hku.hk

human respiratory epithelial cells representing the bronchial and alveolar epithelial cells were developed (Fig 1). The tropism of some emerging infectious respiratory viruses (eg SARS-CoV, avian and human influenza viruses) was investigated using these cultures. The SARS-CoV initiated viral gene transcription and protein synthesis in well-differentiated bronchial epithelial cells only (Fig 2) and showed a productive replication in vitro. In well-differentiated bronchial epithelial cells, type I interferons (interferon-beta) and cytokine and chemokines (eg RANTES, IP-10, IL-6, IL-8, MCP-1, MIP-1α, MIP-2α) were markedly induced after infection with SARS-CoV, compared to human coronavirus HCoV229E and influenza A (H1N1) virus (Fig 3). However, SARS-CoV was unable to infect the alveolar type I-like pneumocytes, but there was a very limited infection and abortive productivity replication of this virus in type II pneumocytes (Fig 1). In an ex vivo experiment for lung culture infection, only the alveolar macrophages were infected with SARS-CoV, whereas alveolar epithelial cells were uninfected.

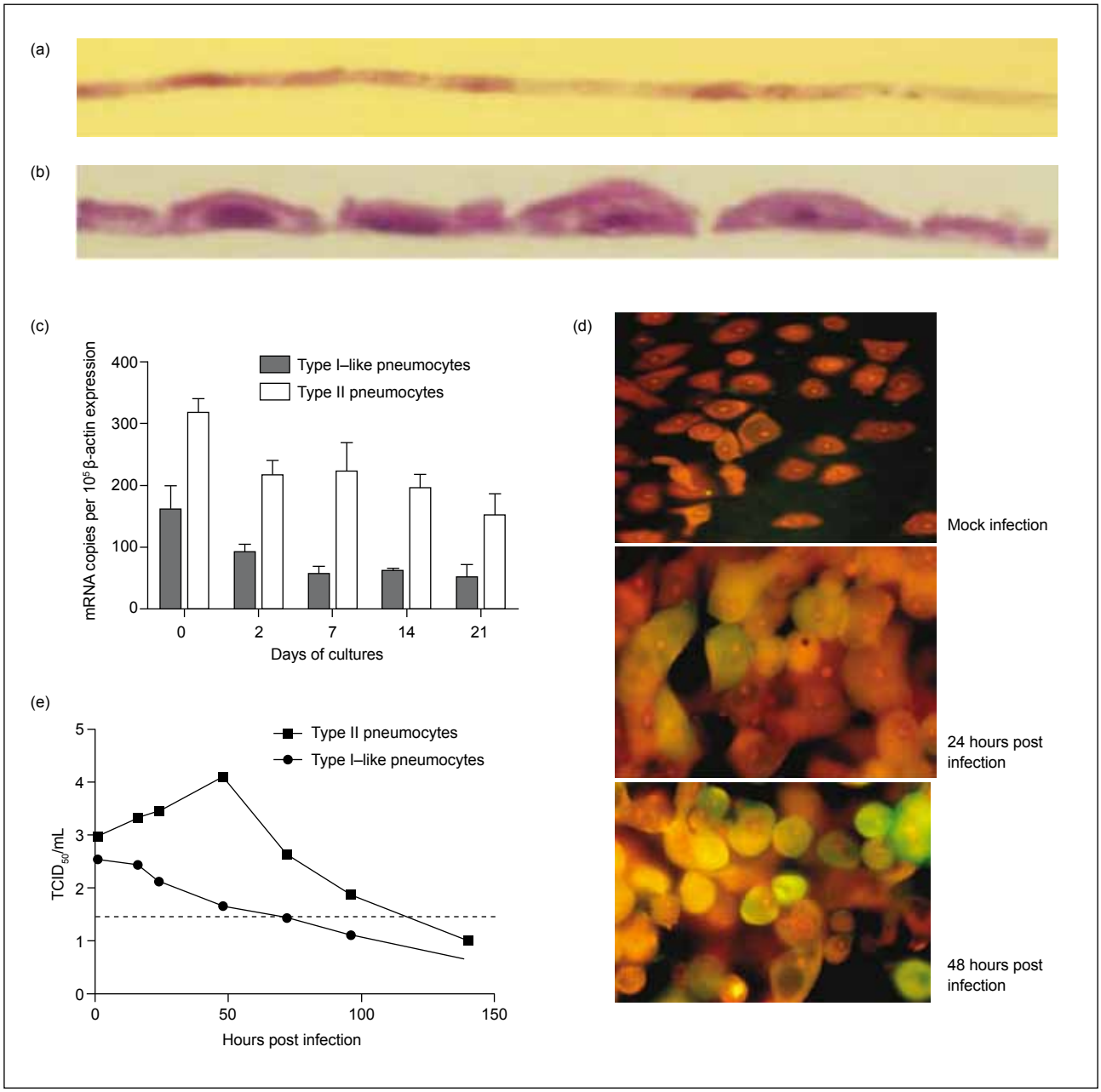

Fig 1. Alveolar (a) type I–like and (b) type II pneumocytes infected with SARS-CoV in vitro by H&E staining. (c) ACE2 mRNA expression of the alveolar type I-like and type II pneumocytes in vitro from day 0 to 21 in culture. (d) Immunofluorescence staining of type II pneumocytes 24 and 48 hours post infection with SARS-CoV and mock infection. The SARS-CoV nucleoprotein was stained green with FITC-conjugated mouse anti-NP protein antibody. (e) The virus titre of the supernatant collected from SARS-CoV–infected type II pneumocytes from 1 to 144 hours post infection

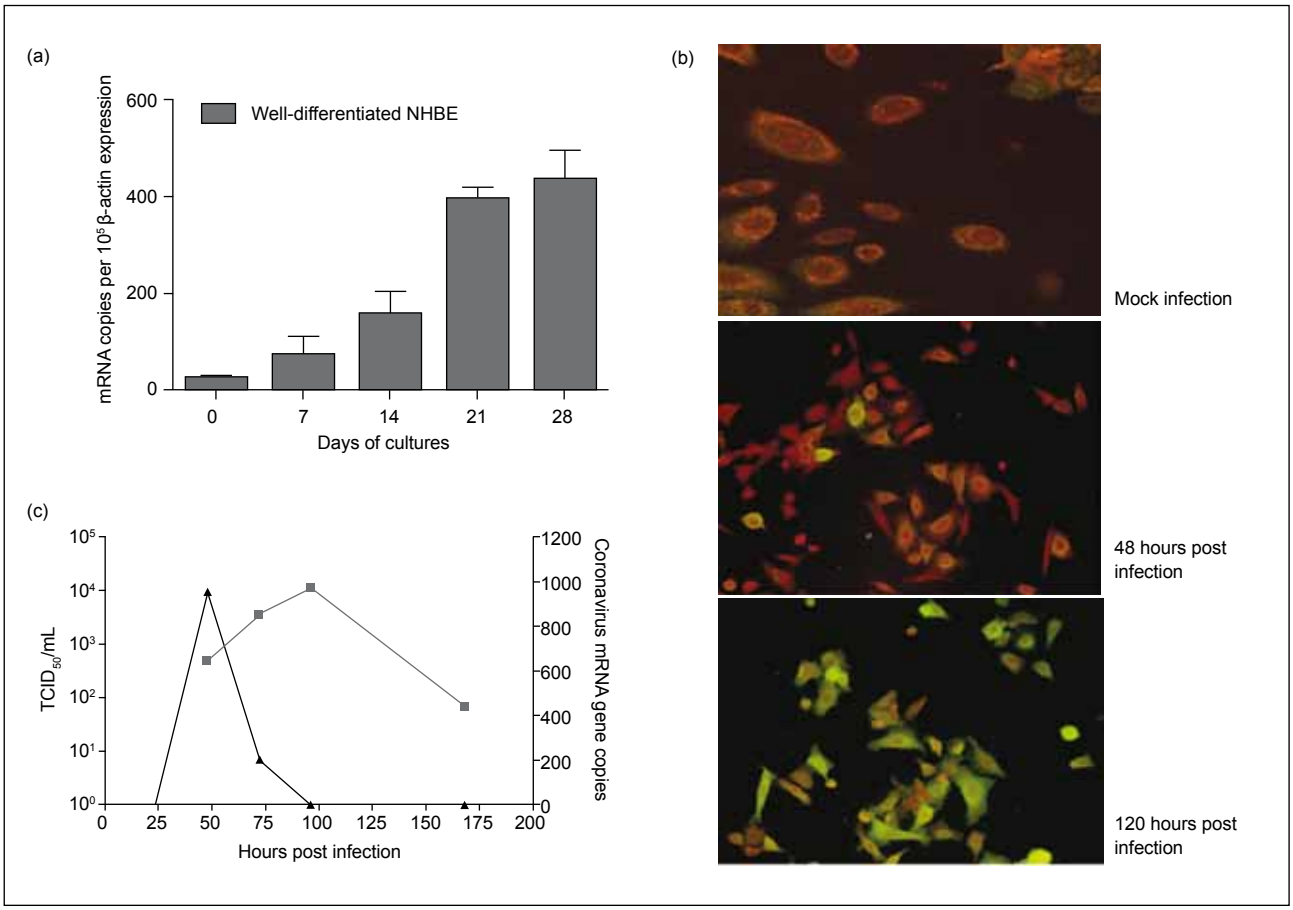

Fig 2. Well-differentiated normal human bronchial epithelial (NHBE) cells in vitro cultured in ALI for 28 days
(a) ACE2 mRNA expression of the well-differentiated NHBE cells from day 0 to 28 in air-liquid interface culture. (b) Immunofluorescence staining of well-differentiated NHBE cells 48 and 120 hours post infection with SARS-CoV and mock infection. The SARS-CoV nucleoprotein was stained green with FITC-conjugated mouse anti-NP protein antibody. (c) The virus titre of the supernatant collected and the mRNA expression of SARS-CoV nucleocapsid gene from SARS-CoV–infected well-differentiated NHBE cells from 1 to 168 hours post infection

Conclusions

Type II pneumocytes and well-differentiated bronchial epithelial cells can be infected with SARS-CoV but in vitro productive infectivity was not shown with alveolar type I-like pneumocytes and non-differentiated bronchial epithelial cells. The in vitro model enables a better understanding of how human respiratory epithelium responds to SARS-CoV and other respiratory viruses in order to better deal with other emerging infections such as avian influenza H5N1 virus. It also helps elucidate the underlying mechanism of inter-species transmission of animal pathogens to humans. Besides, SARS-CoV showed limited tissue tropism for human respiratory tract in vitro (infection and replication demonstrated only in well-differentiated bronchial epithelial cells). Therefore, it is important to use the appropriate in vitro human respiratory model to study the pathogenesis of SARS-CoV.

The host innate immune response induced by the SARS-CoV infection can elicit strong induction of an IFN response in human well-differentiated bronchial epithelial cells. In contrast to the low pathogenicity of HCoV 229E and influenza H1N1 viruses, SARS-CoV can trigger the release of certain cytokines and chemokines in respiratory epithelium. The differential hyper-induction of cytokines plays an important role in human infection with SARS-CoV. Comparison of the gene expression profile of SARS-CoV with the profiles of other highly pathogenic viruses (such as H5N1) may provide further insight into host molecular mechanisms involving viral pathogenicity.

Implications

In vitro and ex vivo studies of the tissue tropism of SARS-CoV can be extended to other emerging respiratory viruses that target human respiratory epithelial cells, especially H5N1 and/or H1N1 viruses. Such studies can be used to characterise and isolate emerging respiratory viruses that are difficult to culture in the laboratory (eg coronavirus HKU1) using transformed cell lines.

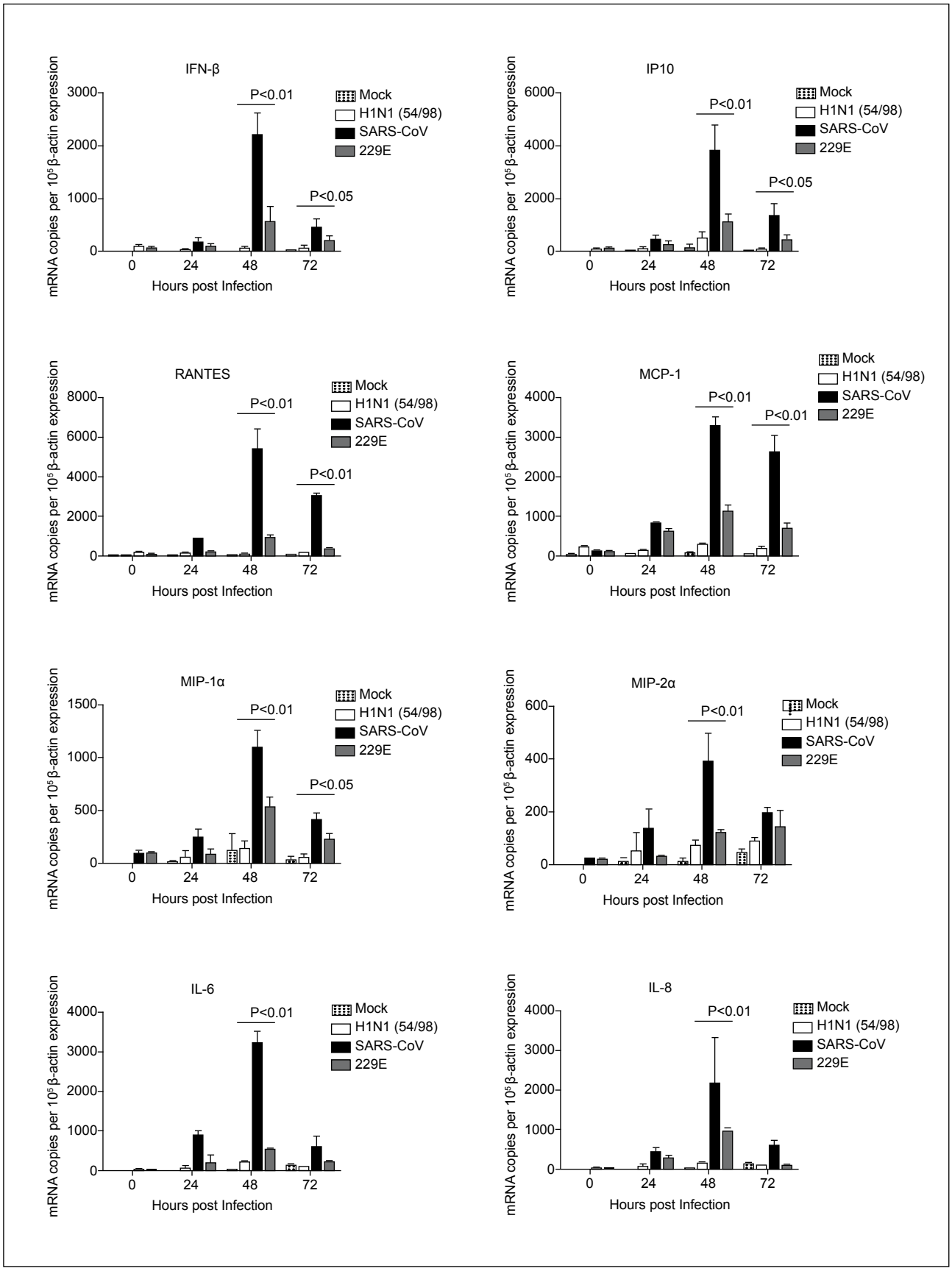

Fig 3. The cytokine and chemokine mRNA expression profile, IFN-β, IP-10, RANTES, MCP-1, MIP-1α, MIP- α, IL-6, and IL-8 gene expression of the well-differentiated normal human bronchial epithelial cells 0, 4, 48, and 72 hours post infection of SARS-CoV, HCoV 9E, and influenza H1N1 virus. The means and standard errors of three representative experiments are shown.

The host innate immune response–related gene expression profiling of respiratory epithelial cells infected with SARS-CoV has provided information about a group of cytokine and chemokine genes that may be involved in its pathogenicity. Our in vitro and ex vivo models enable studying the tropism and pathogenesis of SARS-CoV, especially when suitable small animal models adhering to the 3R principles on the use of animals in research are lacking.

Our study focused on one key component of the innate immune response—the respiratory epithelium. Further investigations of this hypothesis with relevant animal models of SARS could also be considered. In vitro, the SARS-CoV is highly susceptible to the antiviral effects of IFN-ß. In studies on primates, IFN therapy (in combination with steroids) is beneficial for both prophylaxis and early therapy. Our results may provide a biological basis for the observed therapeutic benefit with IFNs in SARS patients when administered early.

Acknowledgement

This study was supported by the Research Fund for the Control of Infectious Diseases (#03040712), Food and Health Bureau, Hong Kong SAR Government.

References

1. Peiris JS, Lai ST, Poon LL, et al. Coronavirus as a possible cause of severe acute respiratory syndrome. Lancet 2003;361:1319-25.
2. Ksiazek TG, Erdman D, Goldsmith CS, et al. A novel coronavirus associated with severe acute respiratory syndrome. N Engl J Med 2003;348:1953-66.
3. Kuiken T, Fouchier RA, Schutten M, et al. Newly discovered coronavirus as the primary cause of severe acute respiratory syndrome. Lancet 2003;362:263-70.
4. Tse GM, To KF, Chan PK, et al. Pulmonary pathological features in coronavirus associated severe acute respiratory syndrome (SARS). J Clin Pathol 2004;57:260-5.
5. Sims AC, Baric RS, Yount B, Burkett SE, Collins PL, Pickles RJ. Severe acute respiratory syndrome coronavirus infection of human ciliated airway epithelia: role of ciliated cells in viral spread in the conducting airways of the lungs. J Virol 2005;79:15511-24.

H Chen 陳鴻霖
Y Guan 管　軼
X Fan 樊曉輝

Animal reservoirs for SARS-like coronavirus in southern China

Key Messages

1. SARS-coronavirus (SARS-CoV) was of zoonotic origin. Wild animals in live-animal markets in Guangdong province were the most likely intermediate hosts and sources of the outbreak in humans. The natural reservoir and emergence pathway of this virus remain largely unknown.
2. Bats appear to be the natural host for coronaviruses, and play a pivotal role in their ecology and evolution.
3. Live-animal markets may have provided an ecosystem that facilitated interspecies transmission of SARS-CoV in Guangdong province.
4. Long-term surveillance of zoonotic pathogens in both humans and animals is important for the prevention of emerging infectious diseases.

Introduction

Severe acute respiratory syndrome (SARS) first occurred in Guangdong province, and subsequently spread to many other countries. A novel SARS coronavirus (SARS-CoV) was the aetiological agent responsible for the outbreak. An investigation of Shenzhen wild-animal markets during the outbreak revealed that SARS-CoV was of zoonotic origin. The outbreak was under control by the summer of 2003, but re-emergence of human infections occurred in December 2003. These cases were again caused by direct transmission from wild animals to humans in the Guangzhou area. Culling of all wild animals in live-animal markets in the Guangzhou area in January 2004 likely averted the second outbreak of SARS in China. We aimed to identify the animal reservoirs for SARS-like CoV and susceptible species that could mediate SARS-CoV transmission to humans.

Methods

This study was conducted from 1 January 2006 to 31 March 2008. Samples collected during the 2003 and 2004 SARS outbreaks were retrospectively analysed. Himalayan palm civets, raccoon, dogs, and other animals in live-animal markets in Guangdong province were the most likely intermediate hosts and sources of the outbreak, but not the natural hosts of SARS-CoV. The natural reservoir and emergence pathway of SARS-CoV remain largely unknown. Molecular epidemiological studies of coronavirus were conducted in wild populations of bats, and also in other wild mammalian animals in live-animal markets in Guangdong during the SARS outbreak (2003/2004) and in Guangxi between 2004 and 2006.[1-3]

Results

Systematic virological surveillances of coronaviruses in bats and other wild animal species were conducted between 2004 and 2007. Approximately 1700 bats were sampled in their natural habitats in 15 provinces of China. In addition, 4420 other mammalian animals belonging to 24 species were sampled in live-animal markets in Guangdong and Guangxi provinces. Bats from 11 of the 15 sampled Chinese provinces tested positive for coronavirus, with an overall detection rate of 4.7% (Table 1). Sequence analysis of the viral genome demonstrated that bats harbour genetically diverse coronaviruses, including some closely related to SARS-like CoV (Fig 1). These findings suggest that bats may be the natural host for coronaviruses and play a pivotal role in coronavirus ecology and evolution.

In live-animal market surveillance, coronaviruses were detected in 81 animals belonging to 10 different mammalian species (Table 2). Phylogenetic analysis of RdRp, Helicase, Spike, Envelope, Matrix, and Nucleocapsid protein genes from these viruses showed that they clustered with the previously known group 1 coronaviruses, suggesting that these coronaviruses are genetically closely related (Fig 2). Further decoding of genome sequences revealed that these viruses share very high amino acid similarity, in some cases even when detected from different host species. This may indicate that these animals were newly infected from a common source inside the live-animal market.

Hong Kong Med J 2011;17(Suppl 6):S36-40

Department of Microbiology, LKS Faculty of Medicine, The University of Hong Kong
H Chen, Y Guan
Department of Microbiology and Immunology, Guangxi Medical University, Nanning, Guangxi ,China
X Fan

RFCID project number: 03040782

Principal applicant and corresponding author:
Dr Honglin Chen
Department of Microbiology, LKS Faculty of Medicine, The University of Hong Kong, Pokfulam, Hong Kong SAR, China
Tel: (852) 2819 9941
Fax: (852) 2855 1241
Email: hlchen@hkucc.hku.hk

Table 1. Coronavirus distribution in different bat species in southern China

Family and species of bat	Common name	No. of samples (No. of coronavirus positive)	Coronavirus group(s)
Rhinolophidae			
Rhinolophus pusillus	Least horseshoe bat	116	-
Rhinolophus malayanus	Malayan horseshoe bat	15	-
Rhinolophus affinis	Intermediate horseshoe bat	79	-
Rhinolophus ferrumequinum	Greater horseshoe bat	41 (4)	1, 4, 5
Rhinolophus thomasi	Thomas's horseshoe bat	14	-
Rhinolophus sinicus	Chinese horseshoe bat	67 (1)	4
Rhinolophus pearsoni	Pearson's horseshoe bat	75 (1)	1
Rhinolophus macrotis	Big-eared horseshoe bat	45 (1)	4
Rhinolophus rex	King horseshoe bat	2	-
Rhinolophus luctus	Woolly horseshoe bat	4	-
Rhinolophus osgoodi	Osgood's horseshoe bat	1	-
Rhinolophus paradoxolophus	Bourret's horseshoe bat	6	-
Rhinolophus rouxi	Rufous horseshoe bat	1	-
Hipposideros armiger	Great leaf-nosed bat	182	-
Hipposideros larvatus	Intermediate leaf-nosed bat	82 (6)	1
Hipposideros pratti	Pratt's leaf-nosed bat	10	-
Hipposideros pomona	Pomona leaf-nosed bat	138 (5)	1
Coelops frithi	East Asian tailless leaf-nosed bat	7	-
Aselliscus stoliczkanus	Stoliczka's Asian trident bat	12	-
Vespertilionidae			
Pipistrellus pipistrellus	Common pipistrelle	27 (6)	5
Pipstrellus abramus	Japanese pipistrelle	41 (14)	5
Pipstrellus sp	-	3	-
Scotophilus kuhlii	Lesser Asiatic yellow house bat	43 (5)	1
Myotis daubentonii	Daubenton's bat	41	-
Myotis mystacinus	Whiskered bat	1	-
Myotis ricketti	Rickett's big-footed bat	56 (14)	1
Myotis chinensis	Large Myotis	3	-
Myotis sp	-	99 (1)	1
Nyctalus aviator	Birdlike noctule	6	-
Nyctalus velutinus	Villus noctule	1	-
Nyctalus noctula	Noctule	17	-
Scotomanes ornatus	Harlequin bat	8	-
Barbastella leucomelas	Eastern barbastelle	1	-
Tylonycteris pachypus	Lesser bamboo bat	14 (2)	5
Ia io	Great evening bat	30 (1)	1
Kerivoula hardwickei	Hardwicke's woolly bat	1	-
Kerivoula sp	-	11	-
Murina leucogaster	Greater tube-nosed bat	5	-
Murina sp	-	4	-
Miniopterus schreibersi	Schreiber's long-fingered bat	135 (17)	1
Miniopterus sp	-	4	-
Pteropodidae			
Cynopterus sphinx	Greater short-nosed fruit bat	11	-
Rousettus leschenaulti	Leschenault's Rousette	31	-
Rousettus sp	-	12	-
Eonycteris spelaea	Lesser dawn bat	3	-
Emballonuridae			
Taphozous melanopogon	Black-bearded tomb bat	181 (1)	-
Megadermatidae			
Megaderma lyra	Greater false vampire bat	2	-
Megaderma spasma	Lesser false vampire bat	4	-
Total	48	1692 (79)	1, 4, 5

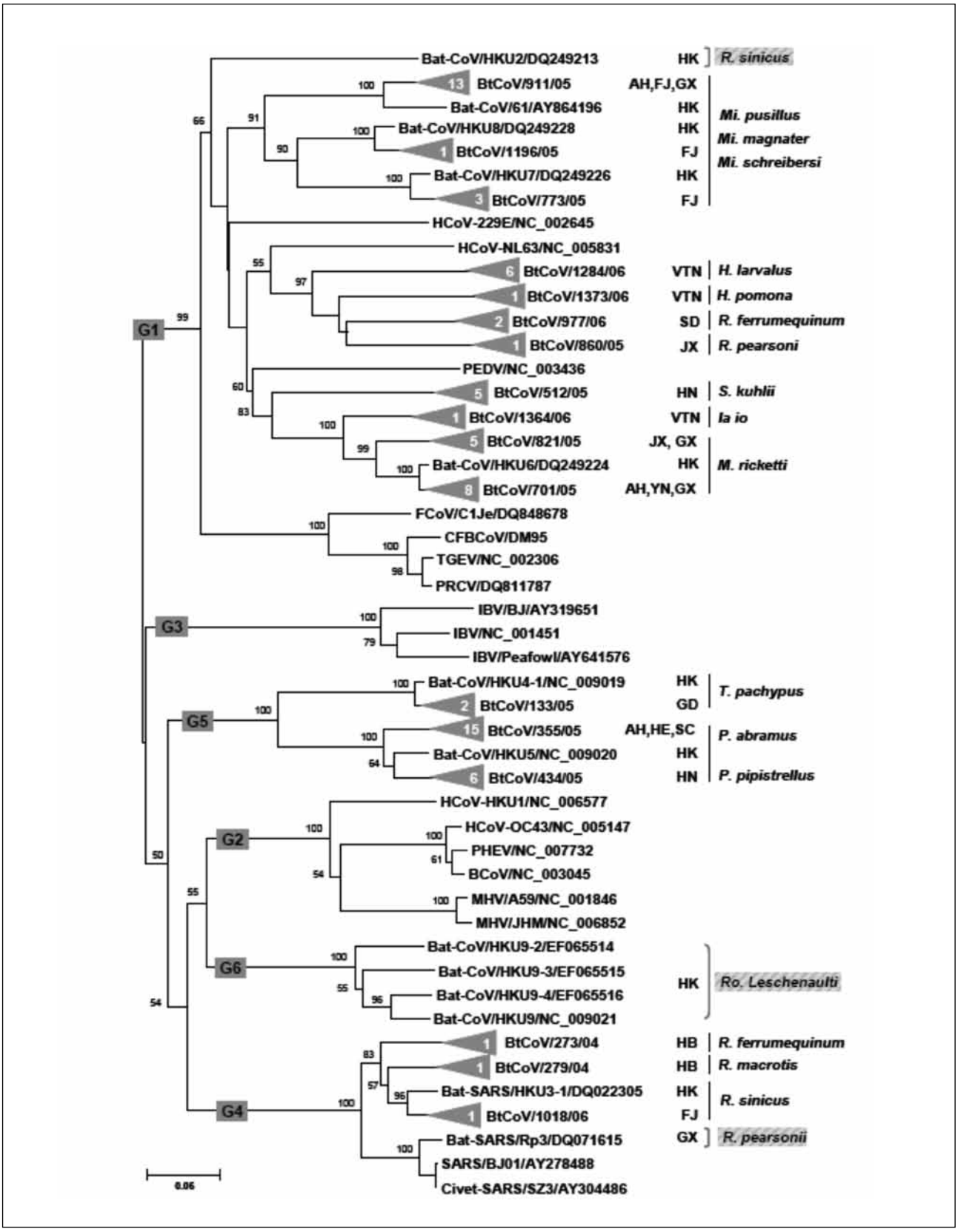

Fig 1. Phylogenetic relationships of coronavirus isolated from bats in China

The tree diagram was based on 440 nucleotides of the RdRp region by the neighbour joining method. Numbers below branch nodes indicate neighbour joining bootstrap values (%), calculated from 1000 bootstrap replicates. Terminal nodes containing bat coronavirus isolated in this study are collapsed and represented by a grey triangle with the number of viruses indicated within. The tree diagram was rooted to Breda virus (AY427798). Scale bar, 0.05 substitution per site. AH denotes Anhui, FJ Fujian, GD Guangdong, GX Guangxi, HA Hainan, HB Hubei, HE Henan, JX Jiangxi, SC Sichuan, SD Shandong, YN Yunnan, HK Hong Kong, and VTN Vietnam

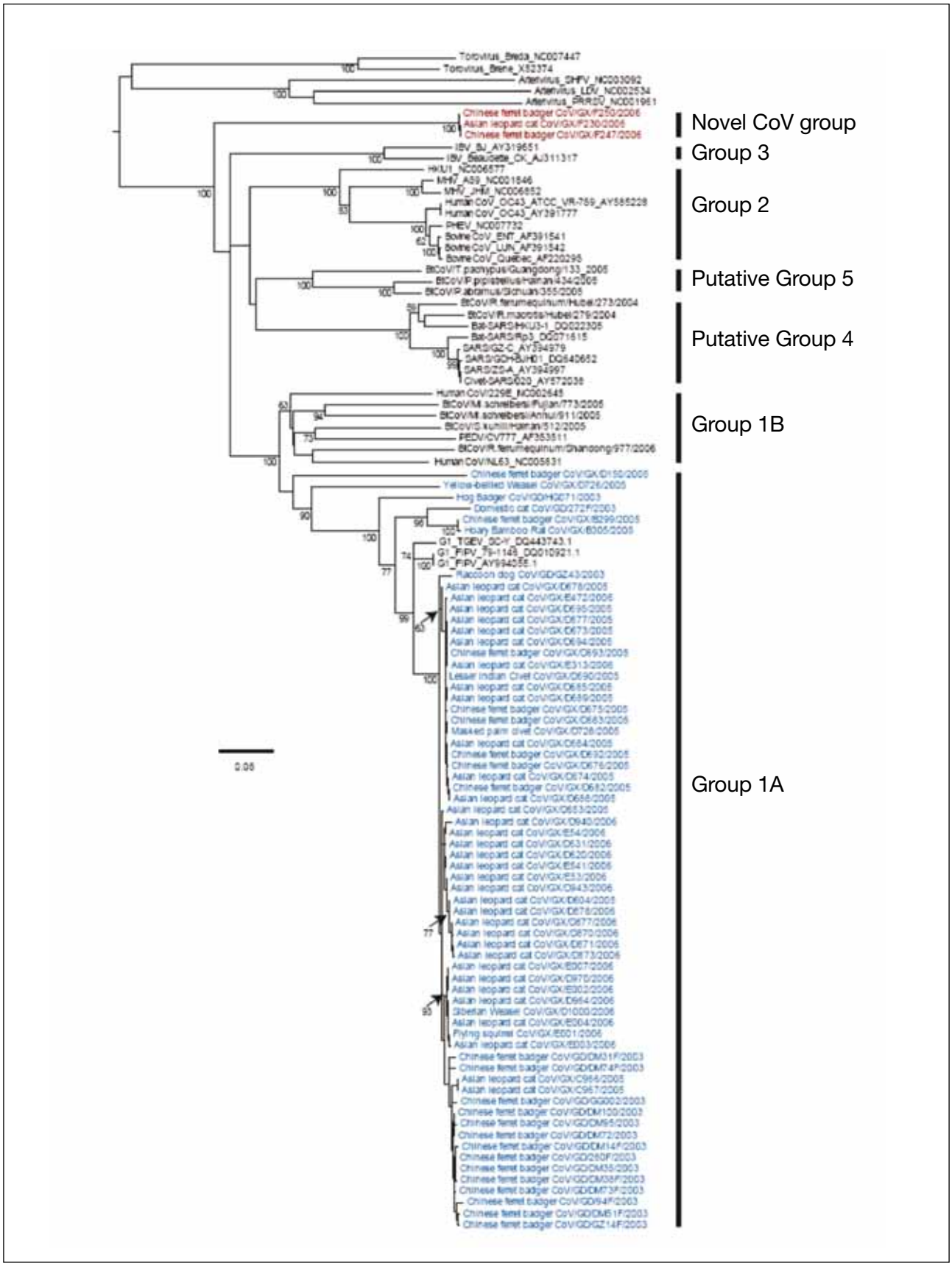

Fig 2. Phylogenetic relationships of coronavirus isolated from wild animals in live-animal markets in China
The tree diagram was based on 440 nucleotides of the RdRp region by the neighbour joining method. Numbers below branch nodes indicate neighbour joining bootstrap values (%), calculated from 1000 bootstrap replicates. The tree diagram was rooted to Gill-associated Okavirus (AF227196)

Table . Coronaviruses detected in wild animals in live-animal markets

Animal species	No. of samples (No. of coronavirus positive)	
	2003/2004	2005/2006
Masked palm civet *(Paguma larvata)*	154	1439 (1)
Hog badger *(Arctonyx collaris)*	49	0
Chinese ferret badger *(Melogale moschata)*	120 (23)	966 (10)
Asian leopard cat *(Prionailurus bengalensis)*	5	1453 (35)
Raccoon dog *(Nyctereutes procyonoides)*	27 (6)	
Hoary bamboo rat *(Rhizomys pruinosus)*	3	108 (1)
Yellow bellied weasel *(Mustela kathiah hodgson)*	0	33 (1)
Lesser Indian civet *(Viverricula indica)*	1	61 (1)
Siberian weasel *(Mustela sibirica)*	0	81 (1)
Flying squirrel *(Petaurista sp)*	0	150 (1)
Sabel *(Martes zibellina)*	0	4
Asiatic brush tailed porcupine *(Atherurus macrourus)*	0	6
Asian small clawed otter *(Aonyx cinerea)*	0	
Crab eating mongoose *(Herpestes urva)*	0	25
Rhesus macaque *(Macaca mulatta)*	19	74
Wild boar *(Sus scrofa)*	1	3
Nutria *(Myocaster coypus)*	5	0
Domestic cat *(Felis catus)*	11 (1)	0
Chinese hare *(Lepus sinensis)*	26	-
Barking deer *(Muntiacus muntjak)*	2	1
Black goat	4	0
Beaver *(Castor fiber)*	6	0
Horse *(Equus)*	10	0
Eurasian badger *(Meles meles)*	14	0
Common pangolin *(Manis pentadactyla)*	6	0
Dog	2	0
Fox	3	0
Chinese pygmy dormouse *(Typhlomys cinereus)*	13	0
Chinese porcupine *(Hystrix hodgsoni)*		0
Swamp deer *(Cervus duvauceli)*	9	0
Total	498 (30)	4420 (51)

Conclusions

Bats appear to be the natural reservoir for coronaviruses (which may serve as precursors for other CoVs, including SARS-CoV) that affect humans and animals. However, the immediate precursor of SARS-CoV remains unknown. Further investigation of coronaviruses in a wider range of bat species and over broader geographical regions is necessary. Many species of wild mammals are susceptible to coronavirus infection. Live-animal markets might have facilitated interspecies transmission of SARS-CoV in Guangdong province during the SARS outbreak. Live-animal markets could pose a significant potential risk for emergence of infectious diseases.

Acknowledgement

This study was supported by the Research Fund for the Control of Infectious Diseases (#03040782), Food and Health Bureau, Hong Kong SAR Government.

References

1. Vijaykrishna D, Smith GJ, Zhang JX, Peiris JS, Chen H, Guan Y. Evolutionary insights into the ecology of coronaviruses. J Virol 2007;81:4012-20.
2. Dong BQ, Liu W, Fan XH, et al. Detection of a novel and highly divergent coronavirus from Asian leopard cats and Chinese ferret badgers in Southern China. J Virol 2007;81:6920-6.
3. Tang XC, Zhang JX, Zhang SY, et al. Prevalence and genetic diversity of coronaviruses in bats from China. J Virol 2006;80:7481-90.

JQ Huang 黃家清
GF Zheng 征革凡
CL Lai 黎青龍
MF Yuen 袁孟峰
BCY Wong 王振宇

Risk of liver cancer in patients with hepatitis B or Ce

Key Messages

1. Among hepatitis B virus carriers, infection with genotype C significantly increases the risk of developing hepatocellular cancer compared to those without this genotype.
2. Among hepatitis C virus carriers, infection with genotype 1b increases the risk of hepatocellular cancer two-fold compared to controls without this genotype.
3. Such increased risk should be explained as risk over and above the existing risk associated with each infection.
4. Hepatitis C virus genotypes 1a and 2a are associated with decreased risk of hepatocellular cancer.

Introduction

Hepatitis B and C are common, serious infectious diseases in both developing and developed countries, affecting over one third of the world's population. The prevalence of hepatitis B seropositivity in the adult population of Hong Kong ranges from 4 to 10%.[1] A significant proportion of these subjects develop chronic hepatitis.[2] It is not clear which of these subgroups of the population are at risk of chronic hepatitis and its complications.

Different genotypes of hepatitis B virus (HBV) or hepatitis C virus (HCV) may play a role in determining which groups of the population are at increased risk of developing hepatocellular cancer (HCC).[3,4] The results remain controversial with regard to which genotype is dominant and the magnitude of the increased risk of HCC (if any).[3,4] Knowing which genotype predisposes patients to HCC can help target populations for monitoring and/or early intervention, so as to achieve an early diagnosis and prolong life.

This study aimed to (1) review the literature on HBV/HCV infection and genotypes and their association with HCC, and (2) estimate the magnitude of risk of HCC associated with HBV/HCV infection and different genotypes.

Methods

This study was conducted from January 2004 to July 2005. A comprehensive computerised literature search was conducted in July 2005 from the databases of MEDLINE, PubMed, EMBASE, and CANCERLIT, using various combinations of the terms: hepatitis, hepatitis B, hepatitis C, hepatitis B virus, hepatitis C virus, HBV, HCV, genotype(s), hepatocellular carcinoma, liver neoplasms, liver cancer, incidence, mortality, death rate, epidemiologic studies, case-control study, and cohort study. Links to related citations were also reviewed to identify other potentially relevant studies. To maximise the yield from the literature search, a manually recursive search of relevant articles, the reference list of retrieved articles, and meeting abstracts was also performed.

Studies included were (1) all observational studies (case-control and cohort) that provide age-matched controls, (2) studies with data on genotypes of HBV or HCV in patients with HCC, (3) documented diagnosis of HCC, and (4) all genotyping methods and all languages. Studies without raw data for retrieval as well as duplicate publications were excluded.

Validity of all included studies was critically appraised, according to the guidelines for reading case-control studies.[5] These guidelines entailed (1) an explicit description of the characteristics of cases and controls, how they were selected, and whether they were matched for age, gender, residence, and other factors; (2) information on the detection of HBV/HCV genotypes and how HCC was diagnosed; (3) data collection, analytic methods, sample size; and (4) the quality of data presentation. This assessment process was conducted by two independent reviewers. As the use of quality scoring in meta-analyses is controversial,[6] no score was given during the quality assessment.

Odds ratios (OR) and 95% confidence intervals (CI) of developing HCC in relation to genotypes of HBV/HCV infection were calculated using either a

Hong Kong Med J 2011;17(Suppl 6):S41-3

Faculty of Medicine, The University of Hong Kong:
Clinical Trials Centre
JQ Huang
Department of Medicine
JQ Huang, GF Zheng, CL Lai, MF Yuen, BCY Wong

HHSRF project number: 01030421

Principal applicant and corresponding author:
Dr Benjamin CY Wong
Department of Medicine, The University of Hong Kong, Hong Kong SAR, China
Tel: (852) 2255 4049
Fax: (852) 2215 3388
Email: bcywong@hku.hk

fixed- or random-effects model, depending on the result of homogeneity tests. Between-study heterogeneity was tested using the Cochran method. A p value of <0.1 was considered statistically significant for the test of homogeneity.

Results

A total of 869 potentially relevant citations were generated; 83 studies were included.

Hepatitis B virus genotypes and risk of hepatocellular cancer

There were 20 case-control and 4 cohort studies (involving 865 cases of HCC and 5858 controls) to provide raw data on the association between HBV genotypes and the risk of developing HCC.

Regarding the HBV genotype A and HCC, 16 case-control and one cohort studies (involving 739 cases and 5002 controls) were analysed. The prevalence of genotype A was 4.74% (35/739) among cases and 5.74% (287/5002) among controls, yielding an OR of 1.29 (95% CI, 0.84-1.97). The test of homogeneity was non-significant (Q Cochran=13.94, df=16, p=0.60). This suggested that patients harbouring HBV genotype A did not confer significant additional risk of developing HCC compared to those carrying HBV alone.

Regarding the HBV genotype B and HCC, 18 case-control and three cohort studies (involving 825 cases and 5426 controls) were analysed. The prevalence of genotype B was 24.6% (203/825) among cases and 25.9% (1406/5426) among controls, yielding an OR of 0.62 (95% CI, 0.45-0.86). This suggested that patients infected with HBV genotype B were at reduced risk of developing HCC compared to those without this genotype.

Regarding the HBV genotype C and HCC, 18 case-control and three cohort studies (involving 825 cases and 5426 controls) were analysed. The prevalence of genotype C was 64.6% (533/825) among cases and 66.7% (3618/5426) among controls, yielding an OR of 1.37 (95% CI, 1.12-1.68). This indicated that patients harbouring HBV genotype C were at increased risk of developing HCC compared to those without this genotype.

Regarding the HBV genotype D and HCC, 11 case-control and one cohort studies (involving 443 cases and 2218 controls) were analysed. The prevalence of HBV genotype D was 9.5% (42/443) among cases and 17.99% (399/2218) among controls, yielding an OR of 0.74 (95% CI, 0.31-1.79). This suggested that HBV genotype D was not related to the development of HCC.

Hepatitis C virus genotypes and risk of hepatocellular cancer

There were 46 case-control and 13 cohort studies (involving 2000 cases of HCC and 10 974 controls) to provide raw data on the association between HCV genotypes and the risk of developing HCC.

Regarding the HCV genotype 1 and HCC, six case-control and three cohort studies (involving 153 HCC cases and 1249) controls were analysed. The prevalence of HCV genotype 1 was 15.0% (23/153) among cases and 39.3% (491/1249) among controls, yielding an OR of 0.77 (95% CI, 0.43-1.40).

Regarding the HCV genotype 1a and HCC, 32 case-control and six cohort studies (involving 1317 cases and 7116 controls) were analysed. The prevalence of HCV genotype 1a was 3.6% (47/1317) among cases and 6.7% (478/7116) among controls, yielding an OR of 0.53 (95% CI, 0.38-0.75). This suggested that patients harbouring the HCV genotype 1a had a significantly lower risk of developing HCC compared to those without this genotype.

Regarding the HCV genotype 1b and HCC, 44 case-control and 11 cohort studies (involving 1962 cases and 10291 controls) were analysed. The prevalence of HCV genotype 1b was 72.3% (1419/1962) among cases and 59.4% (6133/10291) among controls, yielding an OR of 1.97 (95% CI, 1.63-2.37). This suggested that the HCV genotype 1b was associated with a significantly increased risk of developing HCC.

Regarding the HCV genotype 2 and HCC, nine case-control and five cohort studies (involving 185 cases and 1809 controls) were analysed. The prevalence of HCV genotype 2 was 10.6% (44/417) among cases and 10.2% (185/1809) among controls, yielding an OR of 0.721 (95% CI, 0.47-1.096).

Regarding the HCV genotype 2a and HCC, 29 case-control and five cohort studies (involving 1276 cases and 7193 controls) were analysed. The prevalence of HCV genotype 2a was 12.1% (127/1053) among cases and 17.7% (1276/7193) among controls, yielding an OR of 0.78 (95% CI, 0.63-0.96).

Regarding the HCV genotype 2b and HCC, 26 case-control and four cohort studies (involving 275 cases and 5727 controls) were analysed. The prevalence of HCV genotype 2b was 2.9% (34/1174) among cases and 4.8% (275/5731) among controls, yielding an OR of 0.92 (95% CI, 0.67-1.39).

Discussion

Only a minority of patients with HBV or HCV infection develop HCC, despite the high prevalence of such infection. Identifying different genotypes of HBV/HCV helps explain why some patients are prone to developing HCC. No quantitative systematic review of the association between HBV/HCV genotypes and HCC has been published.

Although eight HBV genotypes have been identified, only data for genotypes A to D were adequate for a meaningful meta-analysis. For HBV genotype A, no significantly difference in the sero-frequency was noted. This suggested that genotype A was not common among patients with HBV infection, and not associated with the development of HCC. It neither increased nor decreased the risk of HCC among HBV carriers. For HBV genotypes B and D, they were also not associated with the development of HCC. Patients with HBV genotype C were at increased risk of developing HCC compared to those without this genotype. As HBV genotype C is most commonly found in South East Asia, where the prevalence of HCC is high, the magnitude of risk of developing HCC might have been underestimated due to a high background prevalence of HBV genotype C in HBV carriers without HCC. Therefore, the observed risk ratio of 1.37 should be explained as the risk for HCC over and above any existing risk associated with HBV infection.

The prevalence of HCV infection has increased in the last two decades as a result of increasing rates of drug abuse and transfusion of contaminated blood and blood products. Among HCV-infected patients, only 3.6% of the HCC patients and 6.7% of the controls were sero-positive for genotype 1a. Therefore, the clinical importance of HCV genotype 1a in relation to HCC is unclear. Further studies are needed to examine the clinical importance of this finding. For patients with HCV genotype 1b, they were at increased risk (nearly two-fold) of developing HCC than those without this genotype. A significantly decreased risk ratio was observed for HCV genotype 2a, but not for HCV genotypes 2 and 2b, suggesting that genotypes 2 and 2b had a lesser role, if any, in the development of HCC among HCV-infected patients.

There were several limitations to the current meta-analysis. We focused on individual genotypes and did not take into consideration that patients could have been infected with both HBV and HCV or multiple genotypes. We intentionally broadened the inclusion criteria to maximise the generalisibility of study results. However, cases and controls might not have had comparable durations of infection, which is one of the prognostic factors for HCC development. It is not adequate to examine just one risk factor using multivariate analysis, as HCC is a multi-factorial disease. Although we initially aimed to examine correlations between HBV/HCV genotypes and the incidence and mortality of HCC, the necessary information was not available.

Conclusions

Conflicting reports on the association between these genotypes and HCC make it difficult for clinicians to select which patients to monitor or intervene to prevent the development of HCC. We nevertheless conclude that (1) among HBV carriers, infection with genotype C significantly increases the risk of developing HCC compared to those without this genotype; (2) among HCV carriers, infection with genotype 1b increases the risk of HCC two-fold compared to controls without this genotype; (3) such increased risk should be explained as risk over and above the existing risk associated with HBV or HCV infection; and (4) HCV genotypes 1a and 2a are associated with a decreased risk of developing HCC. However, the clinical importance of these findings remain to be determined.

Acknowledgement

This study was supported by the Health and Health Services Research Fund (HHSRF 01030421), Food and Health Bureau, Hong Kong SAR Government.

References

1. Surveillance of viral hepatitis in Hong Kong - 2001 update, Department of Health, Hong Kong, December 2002.
2. Lai CL. Chronic hepatitis B in Hong Kong: immunisation strategies for the control of hepatitis B virus infection. In: Zuckerman, editor. Hepatitis B in the Asian-Pacific region. Screening, diagnosis and control. Vol. 1. Royal College of Physicians of London; 1997:79-87.
3. Kao JH, Chen PJ, Lai MY, Chen DS. Hepatitis B genotypes correlate with clinical outcomes in patients with chronic hepatitis B. Gastroenterology 2000;118:554-9.
4. Khan MH, Farrell GC, Byth K, et al. Which patients with hepatitis C develop liver complications? Hepatology 2000;31:513-20.
5. Lichtenstein MJ, Mulrow CD, Elwood PC. Guidelines for reading case-control studies. J Chronic Dis 1987;40:893-903.
6. Stroup DF, Berlin JA, Morton SC, et al. Meta-analysis of observational studies in epidemiology: a proposal for reporting. Meta-analysis Of Observational Studies in Epidemiology (MOOSE) group. JAMA 2000;283:2008-12.

NF Ma 馬寧芳
SH Lau 劉思衡
L Hu 胡 亮
SS Dong 董穗穗
XY Guan 關新元

Hepatitis B virus X gene in the development of hepatocellular carcinomae

Key Messages

1. Deletion of the 3'end of the hepatitis B virus X gene (HBx) was frequently detected in clinical hepatocellular carcinoma (HCC) samples.
2. In vivo animal tumour xenograft experiments demonstrated the tumourigenic ability of the C-terminal truncated HBx.
3. cDNA microarray study suggested that the C-terminal truncated HBx played a critical role in the HCC development via activation of cell proliferation and inhibition of apoptosis.

Introduction

Hepatocellular carcinoma (HCC) has been the second commonest cancer in both Hong Kong and China since 1990s. Its overall 5-year survival rate worldwide is about 3%, mainly because of late diagnosis. Although the precise molecular switch that triggers HCC development remains elusive, the aetiological association between hepatitis B virus (HBV) infection and hepatocarcinogenesis has been established.[1] The relative risk of HCC in HBV carriers is 10-fold higher than in non-carriers, but only a small percentage of HBV carriers develop HCC.

One important clue has been derived from the Hepatitis B virus X protein (HBx), which is one of the four proteins encoded by HBV. Previous studies from our group and others have shown that integration of HBV is detected in 80 to 90% of the host genome of HBV-infected HCC cases, and often results in the C-terminal deletion of the protein HBx.[2] Thus, we speculated that truncated HBx may play a role in HCC development.

Frequent C-terminal truncation of hepatitis B virus X protein in hepatitis B virus–related hepatocellular carcinoma

By screening HCC tissue using a microarray containing 194 pairs of HCCs and their matched non-tumour liver tissues, C-terminal truncated HBx was frequently observed in HBV-related HCC tissues. In order to investigate the expression pattern of HBx in HCCs, two antibodies (Ab1 and Ab2) were generated. Their antigen position is shown in Fig. 1a. The antibodies Ab1 and Ab2 can recognise the full-length HBx, whereas the Ab2 cannot bind to the C-terminal truncated HBx. Immunohistochemistry results showed that the C-terminal truncated HBx was detected in 88/111 (79.3%) HCC tissues, whereas full-length HBx was observed in all 111 non-tumour liver tissues, but only in 23/111 (20.7%) of HCC tissues. The corresponding deletion of 3' within the X gene was further confirmed by polymerase chain reaction (PCR) analysis on 20 HCC cases using five pairs of primers encompassing the X gene (Figs. 1b and 1c).

C-terminal truncated HBx enhanced tumour development

We cloned and constructed mammalian expression vectors for ectopic expression of full-length HBx (X2) and C-terminal truncated HBx (X1) in human liver cell lines HepG2 and MIHA. Stable X1-expressing (HepG2-X1 and MIHA-X1) and X2-expressing (HepG2-X2 and MIHA-X2) cell lines were established and tested for their oncogenic ability. MIHA-X1 grew much faster than MIHA-X2 and MIHA-P. The colony formation in soft agar was 10-fold higher in MIHA-X1 than in MIHA-X2 and MIHA-P ($P<0.001$, Student's t test). Tumour xenograft experiment was performed in nude mice to study the tumourigenicity of X1- and X2-expressing cells. Tumour formation in nude mice was observed in 7/10 and 1/10 of nude mice injected with MIHA-X1 and MIHA-X2 cells, respectively. To study the role of HBx in cell apoptosis, a TUNEL assay was employed to compare apoptotic frequencies among X1- and X2-expression cells, as well as vector-transfected mock control cells. Apoptotic frequencies were similar between X1-expression and vector-transfected cells. However, the apoptotic frequency in X2-expression cells was significantly higher than in X1-expression

Hong Kong Med J 2011;17(Suppl 6):S44-7

Department of Clinical Oncology, the University of Hong Kong
NF Ma, SH Lau, L Hu, SS Dong, XY Guan

RFCID project number: 02040162

Principal applicant and corresponding author:
Prof Xin-Yuan Guan
Department of Clinical Oncology, Room L10-56, Laboratory Building, The University of Hong Kong, 21 Sassoon Road, Pokfulam, Hong Kong SAR, China
Tel: (852) 2819 9782
Fax: (852) 2816 9126
Email: xyguan@hkucc.hku.hk

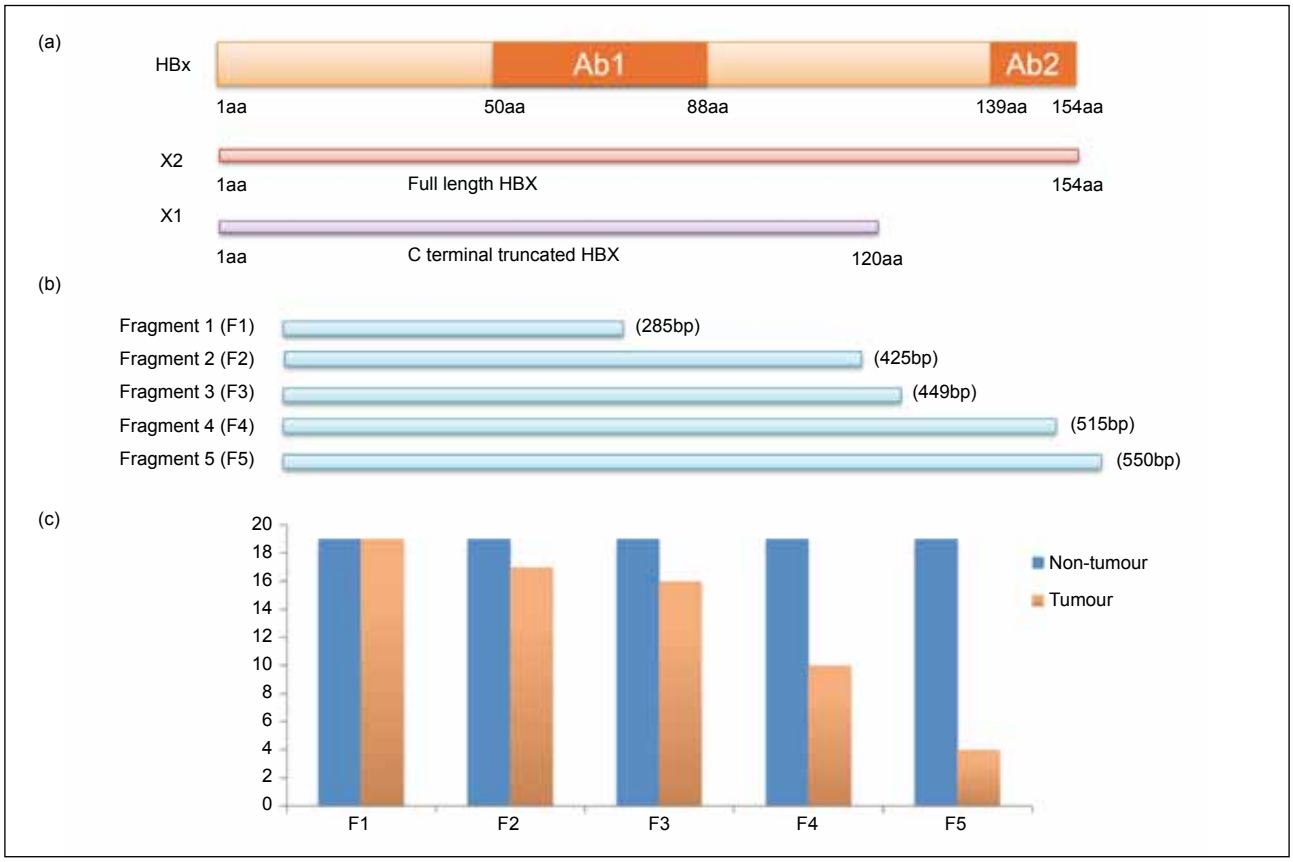

Fig 1. Detection of C-terminal truncation of hepatitis B X protein (HBx) in primary hepatocellular carcinoma (HCC)
(a) Recognition sites of two anti-HBx antibodies (Ab1 and Ab2) on HBx. (b) Polymerase chain reaction (PCR) amplification fragments by five pairs of primers used for detecting 3'-end deletion of X gene. (c) Summary of truncation frequencies in HCC/non-tumour pairs in different regions of HBx

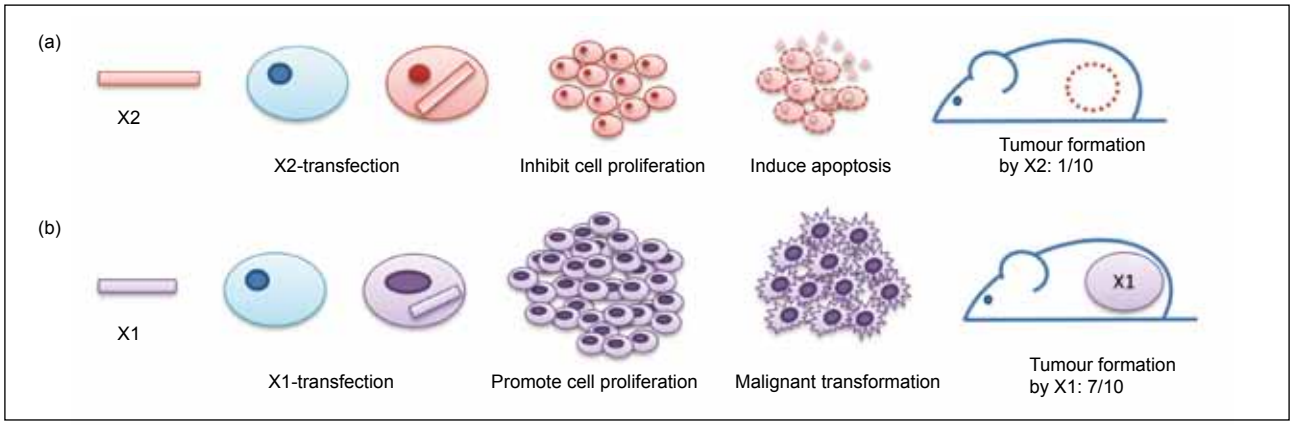

Fig 2. Truncated-X enhanced tumourigenicity
Ectopic expression of X1 and X2 were established in HepG2 and MIHA cells by stable transfections. Ectopic expression of X1 dramatically increased cell growth and colony formation rates, whereas overexpressing X2 inhibited cell growth and induced apoptosis. MIHA-X1 cells were able to promote tumourigenesis in xenograft model

or vector-transfected cells (P<0.001, Student's *t* test). The results are summarised in Fig 2.

cDNA microarray analysis pinpointed key molecules involved in the process

Using a cDNA microarray analysis, we identified the gene signatures contributing to either full-length HBx inducing apoptosis or C-terminal truncated HBx promoting tumourigenicity. Of 12 000 human genes used to compare gene expression profiles between HepG2-X1 and HepG2-X2, 59 genes with significant changes were identified, including 38 genes up-regulated by X1 and 21 genes up-regulated by X2. The most relevant and interesting finding was that genes up-regulated by X1 gene have known functions either promoting proliferation (TFDP1,

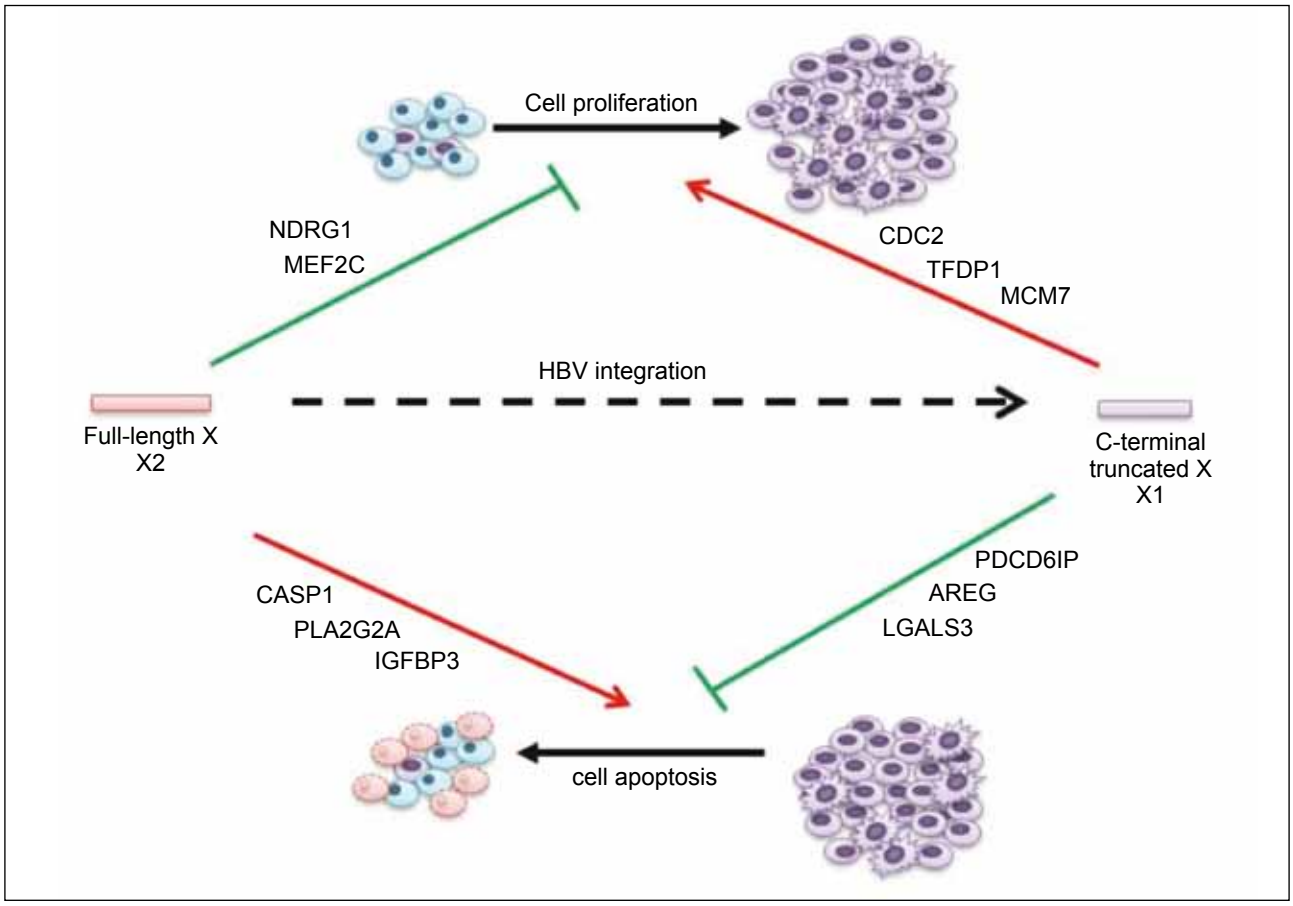

Fig 3. A proposed model for the role of C-terminal truncated hepatitis B X protein (HBx) in hepatocellular carcinogenesis
C-terminal truncated HBx caused by hepatitis B virus (HBV) integration can promote cell proliferation and inhibit cell apoptosis

CDC2, CDC20, CDCA7, and MCM7) or anti-apoptosis (AREG, PDCD6IP, IER3, and LGALS3). In contrast, genes up-regulated by X2 gene have the opposite function like anti-proliferation (MEF2C, NDRG1, and IGFBP3) or pro-apoptosis (CASP1, PLA2G2A, and PLA2G6) [Fig 3].

Discussion

Alteration of HBV X gene has been closely associated with HCC pathogenesis. The mechanism of HBx in HCC development remains unclear. In this study, the C-terminal truncated HBx was frequently detected in HCC tissues (79.3%, n=111), which could also be confirmed by PCR with five pairs of primers encompassing the entire and different lengths of X gene. C-terminal truncated HBx, rather than the full-length HBx, could effectively transform normal liver cell lines and increase the tumourigenicity in cell models by a series of in vivo and in vitro experiments.

HBx plays an important role in HCC pathogenesis by interacting with cellular oncogenes and its functional domain involved in oncogenesis is at the middle of HBx protein. HBx can also induce apoptosis.[3] In the present study, the apoptotic frequency was significantly higher in X2-expression cells than in X1-expression and mock control cells ($P<0.001$). The induction of apoptosis by the full-length HBx, but not by the C-terminal truncated HBx, strongly suggests the C-terminal peptide is required for HBx pro-apoptotic function.

Based on our observations, there are two important functional domains located within the full-length HBx. One is an oncogenic domain (the N-terminal through middle peptide) and the other is a pro-apoptotic domain (the C-terminal peptide). During infection, HBV survival is probably related to a balance between these two functions. When the pro-apoptotic domain is lost, which is probably through viral integration, the balance is broken. Subsequently, the dominant oncogenic domain accelerates the development of HCC.

The hypothesis of two functional domains of HBx protein was supported by our cDNA microarray results, although the molecular mechanism underlining the truncation of C-terminal HBx has yet to be determined. Consistent with the two-domain hypothesis, cDNA array revealed five genes with known functions of promoting cell proliferation were up-regulated in X1-expression cells, and three genes with known negative functions on cell proliferation were down-regulated at least two fold. These results suggest that

the tumourigenic role of the C-terminal truncated HBx is via the activation of cell proliferation and inhibition of cell apoptosis (Fig 3). Our molecular dissections of the two-domain peptides and functions are in progress.

Acknowledgements

This study was supported by Research Fund for the Control of Infectious Diseases (#02040162), Food and Health Bureau, Hong Kong SAR Government. All data of this work have been published on *Clinical Cancer Research* (doi: 10.1158/1078-0432.CCR-07-5082)

References

1. Thorgeirsson SS, Grisham JW. Molecular pathogenesis of human hepatocellular carcinoma. Nat Genet 2002;31:339-46.
2. Wang Y, Lau SH, Sham JS, Wu MC, Wang T, Guan XY. Characterization of HBV integrants in 14 hepatocellular carcinomas: association of truncated X gene and hepatocellular carcinogenesis. Oncogene 2004;23:142-8.
3. Tu H, Bonura C, Giannini C, et al. Biological impact of natural COOH-terminal deletions of hepatitis B virus X protein in hepatocellular carcinoma tissues. Cancer Res 2001;61:7803-10.

AUTHOR INDEX

Published by the Hong Kong Academy of Medicine Press for the Government of the Hong Kong Special Administrative Region. The opinions expressed in the *Hong Kong Medical Journal* and its supplements are those of the authors and do not reflect the official policies of the Hong Kong Academy of Medicine, the Hong Kong Medical Association, the institutions to which the authors are affiliated, or those of the publisher.